

Implausibility of the vibrational theory of olfaction

Eric Block^{a,1}, Seogjoo Jang^{b,1}, Hiroaki Matsunami^{c,1}, Sivakumar Sekharan^d, Bérénice Dethier^a, Mehmed Z. Ertem^{d,e}, Sivaji Gundala^a, Yi Pan^f, Shengju Li^f, Zhen Li^f, Stephene N. Lodge^a, Mehmet Ozbil^d, Huihong Jiang^f, Sonia F. Penalba^a, Victor S. Batista^d, and Hanyu Zhuang^{f,g,1}

^aDepartment of Chemistry, University at Albany, State University of New York, Albany, NY 12222; ^bDepartment of Chemistry and Biochemistry, Queens College, and Graduate Center, City University of New York, Flushing, NY 11367; ^cDepartment of Molecular Genetics and Microbiology and Department of Neurobiology, Duke Institute for Brain Sciences, Duke University Medical Center, Durham, NC 27710; ^dDepartment of Chemistry, Yale University, New Haven, CT 06520; ^eChemistry Department, Brookhaven National Laboratory, Upton, NY 11973; ^fDepartment of Pathophysiology, Key Laboratory of Cell Differentiation and Apoptosis of Ministry of Education, Shanghai Jiaotong University School of Medicine, Shanghai 200025, China; and ^gInstitute of Health Sciences, Shanghai Jiao tong University School of Medicine/Shanghai Institutes for Biological Sciences of Chinese Academy of Sciences, Shanghai 200031, China

Edited by Jerrold Meinwald, Cornell University, Ithaca, NY, and approved March 31, 2015 (received for review February 20, 2015)

The vibrational theory of olfaction assumes that electron transfer occurs across odorants at the active sites of odorant receptors (ORs), serving as a sensitive measure of odorant vibrational frequencies, ultimately leading to olfactory perception. A previous study reported that human subjects differentiated hydrogen/deuterium isotopomers (isomers with isotopic atoms) of the musk compound cyclopentadecanone as evidence supporting the theory. Here, we find no evidence for such differentiation at the molecular level. In fact, we find that the human musk-recognizing receptor, OR5AN1, identified using a heterologous OR expression system and robustly responding to cyclopentadecanone and muscone, fails to distinguish isotopomers of these compounds *in vitro*. Furthermore, the mouse (methylthio)methanethiol-recognizing receptor, MOR244-3, as well as other selected human and mouse ORs, responded similarly to normal, deuterated, and ¹³C isotopomers of their respective ligands, paralleling our results with the musk receptor OR5AN1. These findings suggest that the proposed vibration theory does not apply to the human musk receptor OR5AN1, mouse thiol receptor MOR244-3, or other ORs examined. Also, contrary to the vibration theory predictions, muscone-d₃₀ lacks the 1,380- to 1,550-cm⁻¹ IR bands claimed to be essential for musk odor. Furthermore, our theoretical analysis shows that the proposed electron transfer mechanism of the vibrational frequencies of odorants could be easily suppressed by quantum effects of nonodorant molecular vibrational modes. These and other concerns about electron transfer at ORs, together with our extensive experimental data, argue against the plausibility of the vibration theory.

olfaction | isotopomers | cyclopentadecanone | muscone | electron transfer

In 1870, the British physician William Ogle wrote: “As in the eye and the ear the sensory impression is known to result not from the contact of material particles given off by the object seen or heard, but from waves or undulations of the ether or the air, one cannot but suspect that the same may be true in the remaining sense, and that the undulatory theory of smell. . . [may be] the true one” (1, 2). Of the 29 different “theories of odour” listed in the 1967 edition of *The Chemical Senses* (3), nine associate odor with vibrations, particularly those theories championed by Dyson (4, 5) and Wright (6–8). However, the premise that olfaction involves detection of vibrational frequencies of odorants remains highly speculative because neither the structures of the odorant receptors (ORs) nor the binding sites or the activation mechanisms triggered upon odorant binding to ORs have been established. In 1996–1997, Turin (9–12) elaborated on the undulatory theory of smell, as considered in more detail below, and suggested that a mechanism analogous to inelastic electron tunneling spectroscopy (13) may be involved, where tunneling electrons in the receptor probe the vibrational frequencies of odorants. In 2013, Gane et al. (14) commented that “whether olfaction recognizes odorants by their shape, their molecular vibrations, or both remains an open and controversial

question” and that “a convenient way to address [this question] is to test for odor character differences between deuterated and nondeuterated odorant isotopomers since these have identical ground-state conformations but different vibrational modes.” Gane et al. (14) also stated that a particularly appropriate test case would involve odorants containing “more CH group. . . [such as] musks [which] are among the largest odorants and typically contain 15–18 carbons and 28 or more hydrogens.”

In judging the plausibility of the vibration theory, we use a multipronged approach:

- i) We consider the concepts of shape vs. vibration theory and odorant perception vs. reception.
- ii) As a test of the vibration theory, we have prepared a series of isotopomers of musks and other compounds, containing up to 30 C–H or C–D bonds as test odorants, which are evaluated using *in vitro* activation of receptors identified by us and other groups as being highly responsive to these isotopomers.
- iii) We consider the confounding effects of impurities and isotope effects in interpreting odorant perception, as well as the validity of requirements for specific IR bands for recognition of musks by their receptors.

Significance

The vibrational theory of olfaction posits detection of odorants through their vibrational frequencies rather than solely through “hand-in-glove” substrate/enzyme-like odorant–odorant receptor (OR) interactions. To test the theory, we compare responses of different human and mouse ORs toward deuterated and undeuterated isotopomers (isotopic atom isomers) of receptor-responsive odorants because isotopomers should differ in their molecular vibrational frequencies. However, no differences in receptor response are seen with any tested labeled/unlabeled odorant/receptor pairs. Because published behavioral studies have shown that humans can distinguish isotopomers, per-receptor events or impurities, rather than receptor-level vibrational effects, are suggested. Because theoretical aspects of the vibration theory are also found wanting, the vibration theory is deemed implausible in the absence of compelling receptor-level experimental evidence to the contrary.

Author contributions: E.B., S.J., H.M., V.S.B., and H.Z. designed research; E.B., S.J., H.M., S.S., B.D., M.Z.E., S.G., Y.P., S.L., Z.L., S.N.L., M.O., H.J., S.F.P., V.S.B., and H.Z. performed research; E.B. contributed new reagents/analytic tools; E.B., S.J., H.M., S.S., B.D., M.Z.E., S.G., Y.P., S.N.L., M.O., S.F.P., V.S.B., and H.Z. analyzed data; and E.B., S.J., H.M., V.S.B., and H.Z. wrote the paper.

The authors declare no conflict of interest.

This article is a PNAS Direct Submission.

Freely available online through the PNAS open access option.

¹To whom correspondence may be addressed. Email: eblock@albany.edu, seogjoo.jang@qc.cuny.edu, hiroaki.matsunami@duke.edu, or hanyuzhuang@sjtu.edu.cn.

This article contains supporting information online at www.pnas.org/lookup/suppl/doi:10.1073/pnas.1503054112/-DCSupplemental.

- iv) We examine the physical validity of the models developed to support the vibration theory.
- v) We consider the specific limitations of our in vitro approach using isotopomers to evaluate the vibration theory, based primarily on results obtained with a single identified human musk OR, in addition to other OR/ligand pairs.
- vi) We consider plausible nonvibration theory models for docking of musks to the human musk receptor, OR5AN1, where the musk carbonyl group functions as a hydrogen bond acceptor.

Gane et al. (14) have framed the argument for olfactory discrimination of hydrogen isotopomers as one of “shape” vs. “vibration.” However, neither the binding modes of isotopomers nor their activation mechanisms are known. ORs belong to the superfamily of class A G protein-coupled receptors (GPCRs), which are known to be activated through allosteric conformational changes induced upon ligand binding even without triggering any kind of electron transfer processes. Ligand–receptor interactions can be both attractive and repulsive, involving hydrogen bonding, van der Waals, cation– π , π – π , ion–ion, dipole–dipole, steric, and hydrophobic interactions with the receptor, with water channels and bridging water molecules mediating hydrogen bonds, as well as metal–ion coordination, as we have recently demonstrated in the latter case (15, 16). Therefore, molecular shape can be considered a “straw-man” alternative to the vibration theory when describing the differing affinities of ligands bound to GPCRs (17, 18), including isotopomers (19, 20). Some of these attractive and repulsive interactions were identified in 1940 by Pauling and Delbrück (21), who note that interacting biomolecules “must have complementary surfaces, like die and coin, and also a complementary distribution of active groups.” In addition, shape-related features are misrepresented by vibration theory proponents. For example, Franco et al. (17) stated: “Given that proteins are chiral, a shape-only theory cannot account for the identical odors of most enantiomeric pairs,” echoing similar comments by Turin (22): “One would therefore generally expect enantiomers to have completely different smells. This is emphatically not the case.” However, these assertions are clearly at odds with the highly developed ability of mice and other mammals to discriminate an array of non-pheromonal chiral odorant enantiomeric pairs (23–25), with the divergent in vitro responses to enantiomers by different combinations of ORs (26) and, in particular, with the highly selective response of the musk-sensitive mouse receptor, MOR215-1, to (*R*)-muscone (“*l*-muscone”) compared with (*S*)-muscone (“*d*-muscone”) (27).

In addition to our concerns regarding shape, a second issue relates to describing how different smells are perceived, that is, the perception of an odorant. It is known that in vivo perception of odorants reflects the totality of perireceptor events as well as odorant–OR interactions (reception). Volatile odorants enter the nasal passage, where they dissolve in the nasal mucus overlying the olfactory epithelium and are then rapidly detected by ORs on the cilia of the olfactory sensory neurons, ultimately leading to signaling (28, 29). It is the mechanism of odorant–OR interactions, the reception of the odorant, that we seek to examine with isotopomers to determine whether the vibration theory is plausible, displaying isotope effects, because perception could be influenced by isotope effects due to the perireceptor events involving mucosal components, such as enzymes, mucopolysaccharides, salts, and antibodies.

Whether deuterated and nondeuterated odorant isotopomers can be distinguished by smell and, even if they can, whether this distinction validates the vibration theory is a matter of contention. A 2001 paper by Haffenden et al. (30) reported that benzaldehyde- d_6 gave a statistically significant difference in odor perception relative to normal benzaldehyde, in support of the vibration theory. However, this study has been criticized for

lacking double-blind controls to eliminate bias and because it used an anomalous version of the duo-trio test (31). Furthermore, the study failed to account for perireceptor events, namely, the enzyme-mediated conversion of odorants that has been shown to occur in nasal mucus. For example, benzaldehyde is converted to benzoic acid (32), a reaction potentially subject to significant primary isotope effects (2, 33, 34), which could explain the difference in odor perception for the benzaldehyde isotopomers. Earlier claims that human subjects can distinguish odors of acetophenone isotopomers (9, 35) have been shown to be untrue (14, 31). Recent studies indicate that *Drosophila melanogaster* can distinguish acetophenone isotopomers (36, 37) and that *Apis mellifera* L., the honey bee, can be trained to discriminate pairs of isotopomers (38). These studies differ from earlier insect studies in which isotopomer discrimination was not found. For example, systematic deuteration of 4-(*p*-hydroxyphenyl)-2-butanone acetate, a *Dacus cucurbitae* Coquillett (the male melon fly) attractant, did not affect the attractiveness of the compound to the fly (39); deuteration of alarm pheromones failed to alter the response toward these compounds by *Pogonomyrmex badius* worker ants (40); and honey bees could not distinguish between deuterated and nondeuterated nitrobenzene (41).

Concerns have been raised (42) about aspects of the *Drosophila* study (36), which is “behavioural and not at the receptor level” (2) (also a concern with the *Apis* study). Also, given that the ORs and their downstream signaling in *Drosophila* and humans are completely unrelated, the *Drosophila* study should not be considered predictive of the ability of humans to distinguish isotopomers (2, 17). In view of the above discussion, it is interesting that in a blinded behavioral study, smell panelists distinguished between deuterated and nondeuterated isotopomers of cyclopentadecanone (**1**; Fig. 1A) and other musk odorants (14).

Here, we study the response of human musk-sensitive OR5AN1, identified through screening of heterologously expressed human ORs, to cyclopentadecanone (**1**) and muscone (**4**) isotopomers. We also present pharmacological data on the response of mouse ORs to deuterated and nondeuterated acetophenone and benzaldehyde, as well as selected ^{13}C isotopomers. In addition, we present related studies on the response of various human and mouse ORs to other deuterated and nondeuterated odorants, including (methylthio)methanethiol (MTMT, **8**; Fig. 1C) and bis(methylthiomethyl) disulfide (**9**), studied in connection with our investigation of the role of copper coordination in the recognition of both sulfur-containing odorants by the mouse (methylthio)methanethiol receptor, MOR244-3 (15, 16). Insofar as the ability to distinguish odors of isotopomers directly tests the predictions of the vibration theory, the comparative response of human and mouse ORs to isotopomers of these selected ligands in the heterologous OR expression system constitutes a robust test of the vibration theory. Finally, we discuss the basis for recent vibration theories of olfaction and supporting computational evidence (37, 43–47) in light of well-established electron transfer theories (48). We point out that key assumptions underlying the vibration theory lack experimental support and are missing important physical features expected for biological systems.

Experimental Results

Response of a Human Musk OR to Deuterated and Nondeuterated Muscone and Other Musk Compounds. Because human subjects are reported to discriminate between fully deuterated and nondeuterated cyclopentadecanone (**1**; Exaltone) (14), we sought to perform a corresponding receptor activation assay in vitro.

First, from a commercial sample of cyclopentadecanone (**1**, Fig. 1A), we synthesized **1-d₂₈** (fully deuterated), **1-d₂₄**, and **1-d₄**. Treatment of **1** (twice) with Rh/C in D₂O at 150 °C (49) gave cyclopentadecanol- d_{29} (**2-d₂₉**), which was oxidized with K₂Cr₂O₇/acetone (50) and repeatedly recrystallized to give **1-d₂₈**. Deuterium

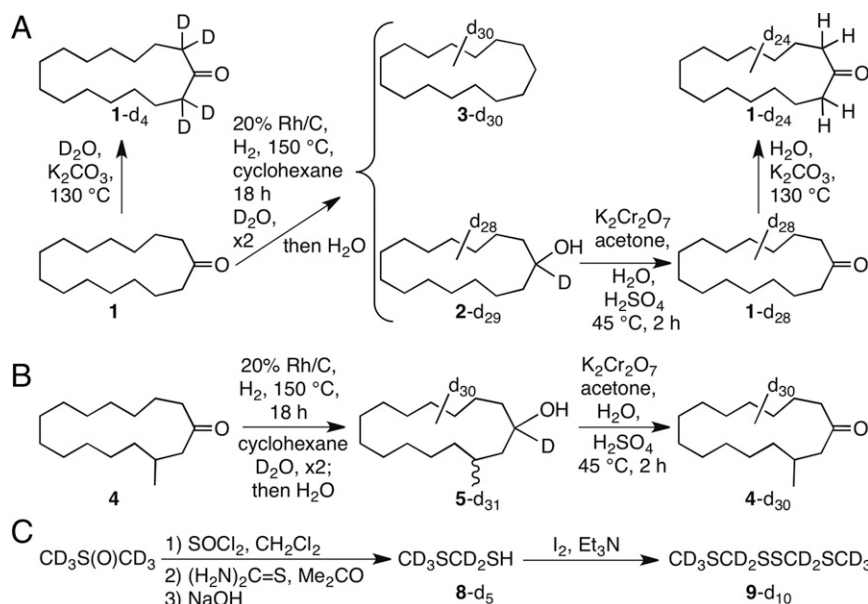


Fig. 1. (A) Preparation of deuterated 1–3. Deuterium could be selectively introduced, or selectively removed, adjacent to the carbonyl group using D₂O/K₂CO₃ or H₂O/K₂CO₃, respectively, at 130 °C; global replacement of all hydrogens could be achieved with Rh/C in D₂O at 150 °C. Repetition led to more complete deuteration as well as reduction of 1 to 3 and 2; oxidation of 2 gave 1 with ~98% deuteration. Chromatography of deuterated 1 with freshly distilled pentane followed by repeated recrystallization from methanol/water to constant melting point gave samples showing no new peaks in their ¹H NMR spectra, other than very weak peaks corresponding to those peaks seen in undeuterated 1. (B) Deuterated (97%) muscone 4 was prepared via alcohol 5 as above. (C) 8-d₅ and 2,4,5,7-tetrathiooctane-d₁₀, (9-d₁₀; 98% deuterium) were prepared as shown. Details of these syntheses are provided in *SI Appendix*.

was selectively introduced into 1, or selectively removed from 1-d₂₈, adjacent to the carbonyl group using D₂O/K₂CO₃ or H₂O/K₂CO₃ (51), giving 1-d₄ and 1-d₂₄, respectively, at 130 °C. A sham sample of 1, which underwent all of the same procedures as 1-d₂₈, but with H₂O instead of D₂O, was also included as a negative control. Both 2-d₂₉ and 3-d₃₀, a byproduct in the catalytic reduction of 1, and nondeuterated 3 were also tested for receptor activation. Similarly, (*R,S*)-muscone [4; (*R,S*)-3-methylcyclopentadecanone] was converted to 4-d₃₀ by way of *cis/trans*-3-methylcyclopentadecanol-d₃₁ (5-d₃₁) (Fig. 1B). Compounds 4 and 4-d₃₀ are baseline-resolved by GC and show very different IR spectra (Fig. 2; experimental details of synthesis and characterization of deuterated compounds 1–5 are provided in *SI Appendix*). Contrary to statements by Gane et al. (14) that a musk receptor “detects vibrations in the 1,380–1,550 cm⁻¹ range,” and that musk odor requires that “the molecule has intense bands in that region,” the IR spectrum of 4-d₃₀ is devoid of 1,380- to 1,550-cm⁻¹ absorption (Fig. 2).

Second, using a heterologous OR expression system (52, 53), we performed parallel screenings of all deuterated and nondeuterated versions of 1 on the human OR repertoire. Among all 330 human ORs screened, we identified one OR, OR5AN1, that is a bona fide receptor for 1 and its isotopomers (*SI Appendix*, Fig. S3.1). OR5AN1 also responds strongly to other related musk analogs, including muscone, cyclopentadecanol, and ω-pentadecalactone (Exatolide) (*SI Appendix*, Fig. S3.3). This response is consistent with a recent report (27), in which OR5AN1 was identified as a human muscone OR, based on homology to the mouse OR MOR215-1, functionally cloned from muscone-responsive glomeruli; a second report on OR5AN1 as the only functional human homolog of mouse muscone ORs in vivo (54); and a third report that only a small number of receptors are thought to be involved in sensing musk odor (55). Our screening and the following confirmation experiments did not reveal any human OR that responded to only one, two, or three of the four isotopomers of 1.

Third, we tested whether or not OR5AN1 responded similarly to isotopomers of the different musk analogs. We found that all

four different isotopomers of 1 gave highly similar responses and the EC₅₀ values of the respective dose–response curves were not significantly different (Fig. 3A, *Left*, and *SI Appendix*, Table S3.2A). In addition, we tested 2 alongside fully C–D deuterated isotopomer 2-d₂₉ and found that even though this compound evoked a much smaller response, similar response levels were seen between the deuterated and nondeuterated versions of this compound (*SI Appendix*, Fig. S3.2B and Table S3.2B). We also found the hydrocarbon analogs cyclopentadecane (3) and 3-d₃₀ to be inactive (*SI Appendix*, Fig. S3.2B). We also tested whether or not OR5AN1 responded similarly to isotopomers of (*R,S*)-muscone (4). Again, we found similar responses between the undeuterated (*R,S*)-muscone and its fully deuterated d₃₀ isotopomer (4-d₃₀) (Fig. 3A, *Right*, and *SI Appendix*, Table S3.2A).

Mouse ORs for Acetophenone and Benzaldehyde Show Similar Responses to All Isotopomers Tested. We assayed isotopomers of acetophenone (6) and benzaldehyde (7) in our system using cognate mouse ORs. Similar to the case of cyclopentadecanone, no significant difference was seen between nondeuterated and deuterated versions for all of the ORs tested (Fig. 4A and B and *SI Appendix*, Table S3.2A). In addition, ¹³C-labeled isotopomers may present a good test for validating/invalidating the vibration theory because they do not significantly alter vibrational frequencies (42). We also included 6-α,β-¹³C₂ and 6-¹³C₈ as well as ¹³CHO-7-¹³C₁ to test against their ¹²C counterparts in our odorant panel. We again found no significant differences among all isotopomers tested (Fig. 4A and B and *SI Appendix*, Table S3.2A), indicating that neither vibrational frequencies nor other factors, such as association/dissociation rates, are contributing to the level of OR activation.

Additional ORs Respond Similarly to Isotopomeric Ligands in Heterologous Cells. We investigated whether other ORs respond differently to isotopomer pairs by assaying 14 other known receptor/ligand pairs using 10 human and mouse ORs and 10 odorous

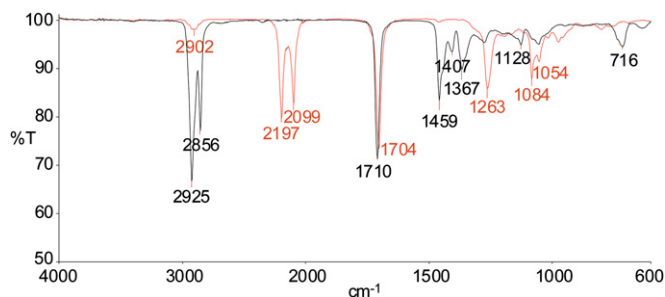


Fig. 2. Superimposed IR spectra of **4-d₃₀** (red trace) and undeuterated muscone (**4**; black trace) showing that **4-d₃₀** is devoid of IR absorption in the 1,380- to 1,550-cm⁻¹ region.

ligands with purchased or synthesized H/D isotopomers, including octanol and octanol-d₁₇, discriminated by *Drosophila* in the aforementioned study (36). Our assay included MTMT (**8**) and MTMT-d₅ (**8-d₅**) (Fig. 1C), as well as bis(methylthiomethyl) disulfide (**9**) and **9-d₁₀**, ligands for mouse receptor MOR244-3, which are notable for requiring copper for ligand binding and whose active site we have modeled (15, 16). Deuterated compound (**8-d₅**) was prepared in several steps from dimethyl sulfoxide-d₆ and then oxidized to **9-d₁₀**; these compounds had ~100% d₅ and d₁₀ deuterium incorporation, respectively, according to GC-MS. When **8** and **9** were tested in the presence of 30 μM Cu²⁺, no differential receptor activity was seen, which was also the case for the other isotopomeric pairs tested (Fig. 3B and *SI Appendix*, Fig. S3.2B and Table S3.2A and B).

Concerns Involving Impurities. When comparing odors of isotopomers, it is essential to ensure that what is being measured is the odor of pure isotopomers devoid of impurities, because trace impurities could lead to a differential response at the organism or receptor level. For example, despite Turin's claims of different odors for deuterated and nondeuterated dimethyl sulfide (35),

no differences were seen in the OR response to dimethyl sulfide (**10**) and **10-d₆** (Fig. 3B and *SI Appendix*, Table S3.2A). These results are consistent with reports that the odor of commercial samples of dimethyl sulfide is due to impurities, which can be removed by washing with aqueous HgCl₂ (56). We suggest that commercial samples of **10-d₆** are of much higher purity than samples of dimethyl sulfide; the former may have lower levels of these impurities. In general, this difference in purity is anticipated between undeuterated and deuterated isotopomers, based on the multistep procedures involved in isotopic labeling and expectations based on the much higher cost of the deuterated compounds.

In a more pertinent example, Gane et al. (14) report the ¹H NMR data for deuterated cyclopentadecanone (**1**), purified by silica gel chromatography using 9:1 hexane/ether, as “δ 2.37 (m, 0.2H), 1.59 (m, 0.22H), 1.30–1.20 (m, 1.72H), 0.84–0.87 (m, 0.25H) [m = multiplet; nH = relative number of protons found by NMR integration, e.g., 0.2H].” Notably, the ¹H NMR spectrum of pure, commercial **1** (fig. 1 of ref. 14 and *SI Appendix*, Fig. S2.7) shows the highest field peak at δ 1.30–1.20, with no evidence of absorption at δ 0.84–0.87, which leads us to question the assertion of Gane et al. (14) for their deuterated **1** that “No impurities are seen in the spectra.” In our hands, the ¹H NMR spectra (*SI Appendix*, Fig. S2.6) for chromatographed and repeatedly recrystallized samples of **1-d₂₈** lack the unidentified impurity peak at δ 0.84–0.87 in the deuterated **1** of Gane et al. (14), which was not seen in the ¹H NMR spectrum of their [or our (*SI Appendix*)] commercial **1**. This impurity peak, seen in our deuterated samples when commercial, unpurified chromatography grade hexanes were used for chromatography, but not with redistilled pentane, could possibly have compromised the smell testing performed by Gane et al. (14), given that for odor evaluation in their study, “after silica gel purification, aliquots of the deuterated musks were diluted in ethanol and their odor character assessed on smelling strips,” and that the δ 0.84–0.87 impurity peak constituted 10% by integration of all residual proton signals. With regard to GC purification before additional smell testing, it is not known whether or not the compound(s)

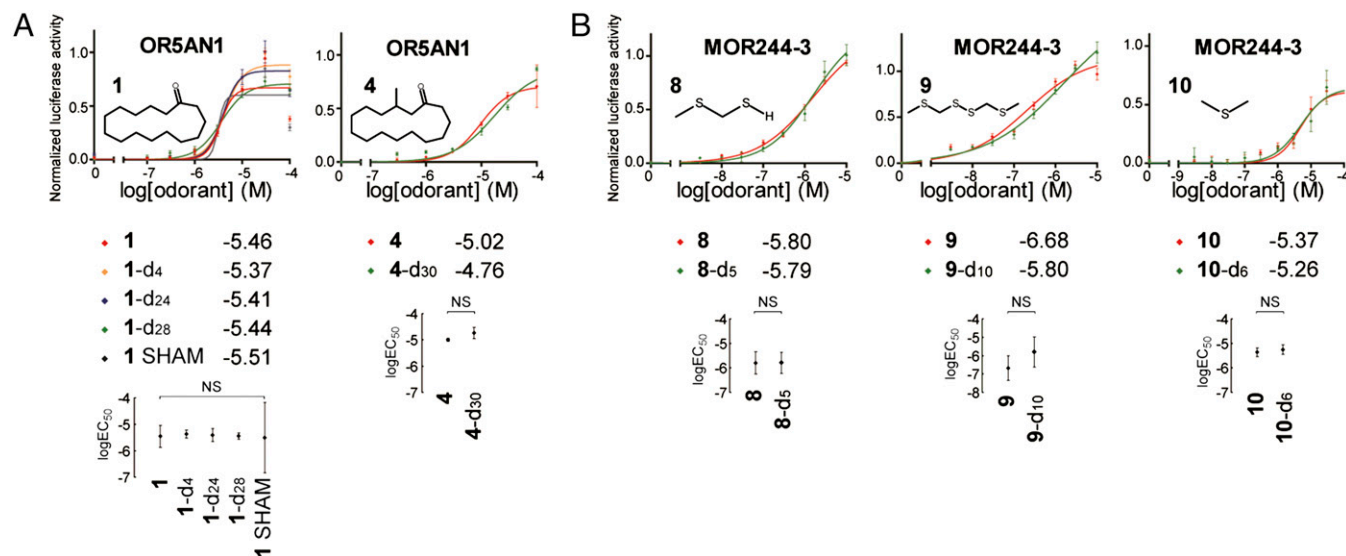


Fig. 3. Dose–response curves of OR5AN1 to isotopomers of cyclopentadecanone (**1**) and muscone (**4**) (A) and MOR244-3 to isotopomers of MTMT (**8**), bis(methylthiomethyl) disulfide (**9**), and dimethyl sulfide (**10**) (B). Best-fit logEC₅₀ values of the curves are shown alongside the graph legends (placed below the graphs). Scatter plots with 95% confidence interval logEC₅₀ values and indicating statistical significances between the logEC₅₀ values among isotopomers are also shown below the corresponding graphs. In B, 30 μM of copper was added upon odorant stimulation. “SHAM” indicates nondeuterated cyclopentadecanone subjected to the same chemical synthetic procedures as the deuterated samples without D₂O addition. NS, not significant. For all dose–response curve graphs, the chemical structures of the respective compounds are shown within the graphs and normalized responses are shown as mean ± SEM (n = 3).

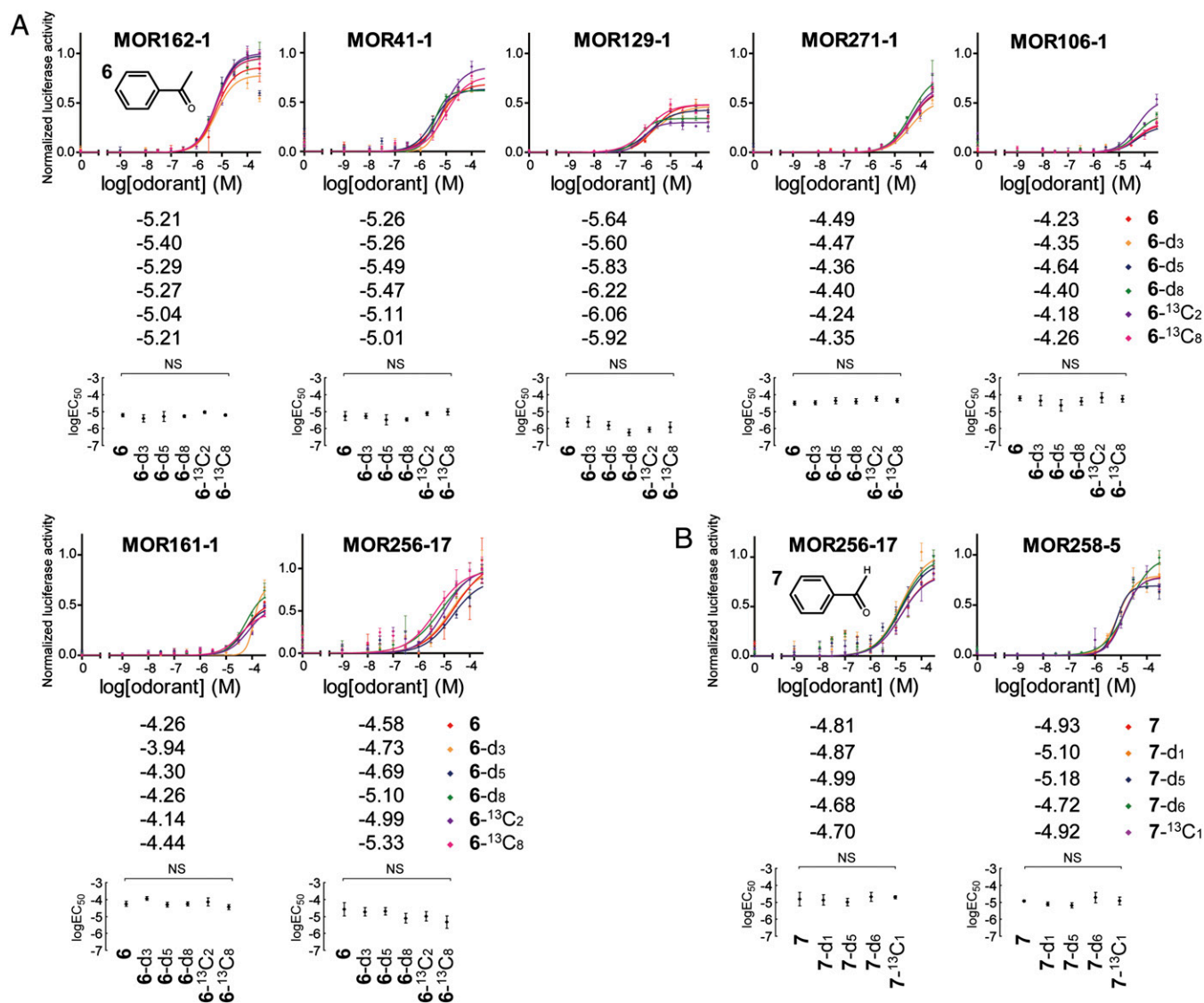


Fig. 4. Dose–response curves of various mouse receptors to isotopomers of acetophenone (**6**) (A) and benzaldehyde (**7**) (B). Best-fit logEC₅₀ values of the curves are shown alongside the graph legends (placed below the graphs). Scatter plots with 95% confidence interval logEC₅₀ values and indicating statistical significances between the logEC₅₀ values among isotopomers are also shown below the corresponding graphs.

responsible for the additional δ 0.84–0.87 impurity peak, or decomposition products of the compound(s) in the hot injection port, coelute with deuterated musks.

Concerns Involving Isotope Effects. Although differences in perception of hydrogen/deuterium isotopomers have been invoked as evidence supporting the vibration theory, it is important to recognize that changing H to D not only changes vibration but also intermolecular interactions, due to the lowering of zero point energy of bonds to D compared with H. Thus, the acidity of D₂O and H₂O are different, hydrogen bonding of O–H and O–D bonds are different, boiling points and freezing points are different, etc. In particular, the gas chromatographic retention times of isotopomeric pairs in the present study are significantly different in all cases examined.

The lack of isotope effects of isotopomers **1–8** when interacting with the corresponding receptors is not unexpected, given that C–H/C–D bonds are not likely to be broken during docking with the receptor. Comparative isotopomer–receptor interactions can be probed computationally. In fact, we have reported a quantum

mechanics/molecular mechanics (QM/MM) model for the mouse OR MOR244-3 in complex with the organosulfur odorant MTMT (**8**) (16). The proposed binding site consists of a copper ion coordinated to the thioether sulfur atom of MTMT as well as to the N, S, and O atoms of H105, C109, and N202 residues. The QM/MM calculations indicate that both the deuterated odorant (**8**-d₅) and nondeuterated odorant (**8**) have similar binding affinities, and that no difference in response is predicted upon deuteration, consistent with the experimental observations (*SI Appendix*).

In addition, we point out that isotope effects in odorant response at the behavioral/organismal level are not necessarily evidence in favor of the vibration theory. Perireceptor events and/or psychophysical processes are known to be important in olfaction (2, 57) and may result in different olfactory percept of isotopomers. For example, it has been proposed that the nasopharyngeal mucus “behaves like a polar chromatographic column” (58), with differential diffusion rates, air/mucus partition coefficients (59), and solubility toward dissolved odorants (60), potentially leading to separation of isotopomers. Because **1** and **1**-d₂₈

are separated by several minutes on a gas chromatographic column (14), and HPLC separation of H/D isotopomers is well known (61), isotopomer fractionation could contribute to perceived differences.

Furthermore, as noted by Brookes et al. (46), biotransformation enzymes reside within the mucus layer and “comparisons of odors could well be affected even by small differences in metabolism, for instance from reaction rates depending on isotope[s].” Because the Baeyer–Villiger (B–V) reaction is known to be mediated (62) by oxidative enzymes (e.g., cytochrome P450), which are present in the nasopharyngeal mucus layer (2, 32, 63, 64), and the B–V reaction of deuterated cyclic ketones forming deuterated lactones is known to show an isotope effect (62), such a reaction might affect odor perception of pairs such as **1** and **1-d₂₈**. Indeed, we have confirmed that **1-d₂₈** undergoes peracid-mediated B–V oxidation faster than nondeuterated **1**, in accord with literature results (62), although a full kinetic analysis in the case of **1/1-d₂₈** was not possible due to partial overlap of ketone and lactone peaks under GC–MS conditions. Deuterium substitution is well known to affect drug pharmacokinetics [e.g., for drugs metabolized by aldehyde oxidase (65)], and can change many intermolecular interactions.

Critique of Current Theoretical Proposals. Turin’s idea that electron transfer occurs at ORs and that these ORs can detect odorant vibrational frequencies has gained traction in recent years (37, 43–47). These theoretical works (37, 43, 47) are in support of the vibration theory but remain largely tentative because they admittedly rely on unconfirmed assumptions, lacking experimental evidence, to make the proposal appear to be feasible. Electron transfer in biological environments is not uncommon. There is a substantial amount of literature reporting various experimental and theoretical studies. However, no evidence exists that GPCRs require electron transfer for their activation. The proposed mechanism (43) of delivering electrons to ORs is also too unreliable to set the stage for a failsafe mechanism of detecting odorants’ vibrational frequencies. In addition, biological electron transfer processes are sensitive to chemical bonding characteristics, local molecular environments, and dynamic fluctuations, which can affect the transfer rate by orders of magnitudes. OR sites are floppy and open to numerous and diverse-sized odorants, and they are susceptible to these effects. Current theoretical proposals supporting the vibration theory, as summarized below, are oblivious to these complex issues.

Brookes et al. (43) proposed a model based on the standard spin-boson type of Hamiltonian for electron transfer (66), using Jortner’s expression (67) of electron transfer rate for quantum vibrational modes. Two electron transfer times, τ_0 for electron transfer without odorant and τ_1 for electron transfer exciting one vibrational quantum of the odorant, were introduced. Assuming that all vibrational modes coupled to electron transfer are classical, except for the odorant oscillator, they obtain Marcus’s expression (68) for $1/\tau_0$ and Jortner’s expression (67) for $1/\tau_1$ (SI Appendix). Approximating the odorant oscillator as a classical point dipole, they estimated the Huang–Rhys factor of the odorant oscillator to be $S \approx 0.01$. This value is very small, and would be difficult to detect unless high-quality samples and sensitive spectroscopic techniques are used. Brookes et al. (43) recognize this issue and propose that (i) an OR site is finely tuned so that the energy difference between the electron donor and acceptor matches the vibrational quantum of the odorant oscillator, $E_D - E_A = \hbar\Omega$, and (ii) the reorganization energy of the protein environment is assumed to be very small, *ca.* $\lambda = 30$ meV. Under these conditions, they conclude that electron transfer could detect odorant vibrational frequencies.

Although Brookes et al. (43) bring the vibration theory to a more concrete theoretical level, none of the key assumptions has supporting experimental evidence. Furthermore, their estimate for the reorganization energy of the electron transfer-coupled protein environment is unusually small even compared with

other confirmed biological electron transfer processes (69). The reorganization energy for electron transfer in well-secured hydrophobic pockets of proteins can be small (70), but the assumed value (43) relies on old literature data (71), which is smaller by an order of magnitude than more recent estimates (72). Although the restriction on the reorganization energy can be relieved somewhat by modification of the resonance condition (SI Appendix), Solov’yov et al. (47) estimate that the reorganization energy needs to be smaller than 0.1 eV for the vibration theory to be feasible. This value is still substantially smaller than commonly known values (69, 70). Clear experimental or computational evidence supporting such estimate is lacking.

Another fundamental issue with the proposed theoretical models (43, 47) is the neglect of quantum contributions from molecular vibrational modes other than those molecular vibrational modes of the odorant oscillator, leaving the window of vibrational frequencies open only for odorant molecules. This is tantamount to neglect of molecular-level structural information on OR sites available from homology models (47). The metal–ligand bonds and peptide bonds in the postulated electron-donor or acceptor sites could have similarly high-frequency modes with inelastic effects at least comparable to those high-frequency modes of odorants. Full consideration of such modes can easily alter the qualitative nature of electron transfer (73, 74) and could mask the vibrational frequencies of odorants, as illustrated in Fig. 5, making a cursory analysis of the vibration theory highly unreliable (a more detailed description is provided in SI Appendix).

The resulting values of detection efficiency τ_0/τ_1 , plotted in Fig. 5, show that a modest amount of coupling to quantum vibrational modes of the environment could be sufficient to suppress the proposed odor detection mechanism of the vibration theory (43). In addition, considering the prevalence of C–H bonds in protein environments, it is unclear how the effects of deuterating the odorants, as proposed by Gane et al. (14), can stand out even if the proposed electron transfer mechanism were

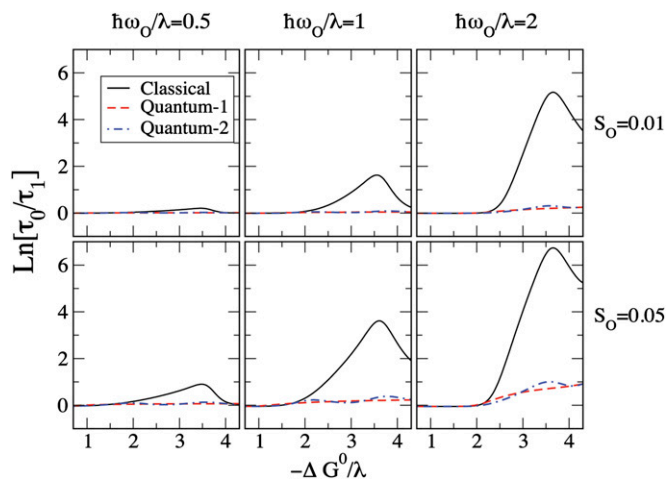


Fig. 5. Natural logarithms of the ratios of τ_0/τ_1 vs. $-\Delta G^0/\lambda$ (negative Gibbs free energy of reaction in the unit of reorganization energy) corresponding to the results in SI Appendix, Figs. S1.1–S1.3. The term “Classical” refers to the classical limit of Ohmic bath, SI Appendix, Eq. 18, with parameters for SI Appendix, Fig. S1.1. The term “Quantum-1” refers to the quantum regime of the Ohmic bath with parameters for SI Appendix, Fig. S1.2. The term “Quantum-2” refers to the case of classical Ohmic bath plus one quantum mode in the bath with parameters for SI Appendix, Fig. S1.3. Each column represents a different value of $\hbar\omega_0/\lambda$, where ω_0 is the angular frequency of the odorant oscillator and λ is the reorganization energy of the protein environments. $S_0 = 0.01$ (Upper) and $S_0 = 0.05$ (Lower), where S_0 is the Huang–Rhys factor for the odorant oscillator.

true. Although Solov'yov et al. (47) made significant improvements to the work by Brookes et al. (43) by including the effects of more than one vibrational mode of odorants, calculating the Huang–Rhys factor in the presence of the field, and recognizing the importance of structural fitting of odorants, they also omitted consideration of nonodorant quantum vibrational modes. Thus, the issues raised above remain unresolved.

Bittner et al. (37) proposed a model where the electron transfer can occur only through the odorant as a bridge. The sensitivity to molecular vibration in this model also originates from resonance effects, assuming that internal modes of the odorant are excited impulsively during hole transfer from a donor site to acceptor site on the OR, along the direction of the gradient of the Born–Oppenheimer potential for its oxidized form. These assumptions lead to an interesting expression for the detection efficiency with direct correlation to IR signals and with some predictive capability. However, the final rate expression does not depend on the electronic energy of the odorant, which is at odds with most known multistate electron transfer processes (75). Most importantly, the model does not include the reorganization energy in the resonance condition, let alone the effects of quantum vibrational modes of donor and acceptor sites.

Other important issues that are not considered by all current theoretical proposals are the effects of disorder, dynamical fluctuations, and the sensitivity of electron couplings to bonding characteristics. For example, it is well established (75) that effective donor–acceptor electronic coupling is very sensitive to chemical characteristics and conformational details of the bridge (odorant) molecules [e.g., as shown by recent single-molecule conductance measurements, where substantial fluctuations of conductance were seen even when metallic electrodes are used under well-controlled bias potentials (76)]. Dynamical modulation of these electronic couplings is also very likely, resulting in fundamentally different kinetics (77, 78). Therefore, all of these factors can easily alter the electron transfer rate by orders of magnitude, becoming as important or more so, than the proposed Jortner-type vibronic effect (43). A theory that can genuinely support Turin's idea needs to demonstrate that electron transfer can indeed amplify small vibrational contributions of odorants despite all of these complicating effects typical of electron transfer in biological environments.

Discussion

In the absence of OR structural models, theoretical work is limited to the construction of phenomenological models consistent with available experimental observations. The principal experimental evidence supporting the vibrational theory has been the deuterium isotope effect at the perceptual (behavioral) level (14, 36, 38). However, we find no experimental evidence supporting the theory at the molecular level. We focused on the functional analysis of a human OR tuned to the same musk compounds that were recently promoted as important experimental evidence, with the aim of specifically testing the electron tunneling mechanism at the receptor level. However, the experimental data reported in our study show a dramatic lack of correlation between OR-level signals and isotope effects over an extended set of 26 receptor/ligand pairs, with at least one deuterated counterpart to each of these ligands. In addition, we find that the assumptions of current theoretical models lack experimental support and do not necessarily fit into the general picture of typical electron transfer processes in biological environments. Thus, our combined experimental results and theoretical analysis present a comprehensive set of observations questioning the validity of the vibration theory as a plausible description of odor detection.

Gane et al. (14), finding that cyclopentadecanone (**1**) and **1-d₂₈** can be distinguished by human smell, speculated that “a small number of receptors, possibly just one, are involved in sensing

musk odor,” in accord with an earlier similar conclusion (55). A recent study (27) using heterologous cell assays and a c-fos induction assay in the olfactory bulb identified MOR215-1 as a strong musk-responding mouse OR. This study observes that “6% of humans are muscone anosmic...; therefore, muscone may be recognized by only a small set of ORs, including OR5AN1 in humans, and genetic variation in these receptors may cause muscone anosmia” (27). McClintock et al. (54) identified five highly related ORs, including MOR215-1, that are likely to be activated by muscone in freely behaving mice, supporting multiple muscone receptors. Importantly, however, the only functional human counterpart of these ORs is OR5AN1. Here, we identify OR5AN1 through a thorough screening of the human OR repertoire using all four isotopomers of **1** and find that this OR responds similarly to these isotopomers. In summary, despite extensive screening, multiple research groups have identified only OR5AN1 as a human musk receptor. Nevertheless, failure to identify other human musk receptors in addition to OR5AN1 still leaves open the possibility that there are other human musk ORs. Future studies with genetic association with the OR5AN1 locus and/or development of OR5AN1-specific antagonist(s) could show whether OR5AN1 is the only OR that mediates behavioral responses to the musk compounds.

We supplement our study of the response of OR5AN1 to isotopomers with the analysis of the response of copper-requiring mouse receptor MOR244-3 to isotopomers of its most active ligands, as well as with the study of several other human and mouse receptors responding to cognate ligands. The consistent lack of difference found in the responses of all of these human and mouse receptors to isotopomers lessens our concern about possibly missing key receptors that are differentially responsive to isotopomers. Furthermore, we note it would be unusual for some, but not all, ORs strongly responsive to a particular ligand to demonstrate isotope discrimination.

In addition to OR5AN1, we describe here OR/ligand pairs of isotopomers of compounds **6–9**. We found that none of the tested receptors exhibits different responses to isotopomers, although the IR spectra of the nondeuterated parents are strikingly different from the fully deuterated analogs (Fig. 2 and *SI Appendix*), and the inelastic electron-tunneling vibration frequencies would also be expected to differ significantly. Our experiments sought to examine the validity of the vibration theory at the receptor level by comparing the differential response to isotopomers, using a cell-based OR expression system, compared with differential responses found from animal behavioral studies or human odorant perception. So far, many studies have been able to correlate functional responses from intact neurons to functional responses of *in vitro* OR pharmacology. For example, by comparing the response profiles of several mouse ORs to cognate ligands using functional imaging of the olfactory bulb against heterologous ORs, Oka et al. (79) showed that ligand selectivity of the ORs is comparable, although the responses vary in efficacy. In addition, *in vitro* activity of human receptors in heterologous cells has been shown to predict human perception for several different ORs, also suggesting that the heterologous system at least partly mimics *in vivo* function (80, 81). Nonetheless, it should be noted that the current *in vitro* method is not without limitations. The experimental setup may lack the source of electrons assumed in the vibration theory. We cannot exclude the possibility that some ORs simply may not function in our system, thus reflecting only a fraction of OR responses that may be present at the perceptual level. One possibility is that the activation of certain ORs may lead to alternative signaling pathways and that our cAMP-based assay may not be able to detect such activation. In addition, the absence of a nasal mucosal environment prevents the evaluation of the significance of perireceptor events.

With the limitations noted above, given the absence of an effect of deuteration on OR response, as demonstrated in the present work, and the lack of experimental evidence supporting the fundamental assumptions of current theoretical models of the vibration theory, we conclude that the perceived differences in smell and olfactory response are likely due to perireceptor processes or impurity of the tested odorants and not to inelastic electron tunneling assisted by vibrational modes.

Conclusion

Since Ogle's original proposal (1) for the vibration theory more than 140 y ago, the idea has been embraced by Dyson (4, 5), Wright (6–8), and Turin (9, 10). However, we find that it does not apply to the human musk receptor OR5AN1 or the mouse thiol receptor MOR244-3, as shown by the clear absence of isotope effects with deorphaned human and mouse ORs on exposure to the specific deuterated, ^{13}C , and nonlabeled ligands for these ORs. Our testing included OR5AN1, which strongly responds identically to both muscone (4) and 4-d $_{30}$. We also find that 4-d $_{30}$ lacks IR absorption in the 1,380- to 1,550-cm $^{-1}$ range (Fig. 2), which is clearly at odds with the claims of Gane et al. (14) that a musk receptor “detects vibrations in the 1,380–1,550 cm $^{-1}$ range,” and that musk odor requires that “the molecule has intense bands in that region.” Muscone-d $_{30}$ has even more C–D bonds than found in ligands previously tested by Gane et al. (14), who claim that it is the number of hydrogen vibrational modes that is “essential for detecting the difference between isotopomers.”

Our experimental results are consistent with the ability of mice (and other mammals) to discriminate between a large array of nonpheromonal chiral odorant enantiomeric pairs, as well as with the ability of mouse receptor MOR215-1 to discriminate (*R*)- and (*S*)-muscone (27). Although it is known that the muscone enantiomers “differ from each other with regard to odor quality and the odor detection threshold in humans” (27), data are not yet available on the response of OR5AN1 to muscone enantiomers. We agree with the suggestion that the “muscone receptor is specific to C15 and C16 macrocyclic ketone compounds and that the ketone moiety may function as a hydrogen bond acceptor” (27). Although QM/MM and mutagenesis studies should elucidate the nature of the interaction of musks with OR5AN1, such a suggestion would be in accord with specific hydrogen bonding interactions as observed for the mouse eugenol receptor mOR-EG (82), as well as our observation that hydrocarbon analog cyclopentadecane (3), which lacks the carbonyl group of 1, is inactive toward OR5AN1 (*SI Appendix*, Fig. S3.2B).

Although some insect and human behavioral/psychophysical studies showed perceptual differences for isotopomers, perireceptor events or trace impurities may be sufficient to explain any isotope effect (2). Finally, with regard to the plausibility of the vibration theory, it has been argued that rather than being causal, any nonisotopic relationship between vibrational frequency and odor may come about indirectly as a consequence of

“similar molecules having similar properties” (83) and because “the vibration spectrum of a molecule reflects its structure” (84). Our findings that the vibration theory is not supported by rigorous analysis of the response of OR5AN1 to diverse isotopomers reinforce Sell's recommendation (85) that those individuals “wishing to study the nature of odorant-receptor recognition should use receptor activation rather than odor as input data.”

Materials and Methods

Chemicals. All odorants were purchased from Sigma–Aldrich, J&K, or Chemsky, or were synthesized in-house. Deuterium incorporation into compounds 1–4, 8, and 9 was accomplished by methods reported in the literature from undeuterated or deuterated commercially available starting materials, as described in *SI Appendix*, with full characterization of all compounds, following purification by chromatography and recrystallization to a constant melting point (when possible), by ^1H and ^{13}C NMR, IR spectroscopy, and GC-MS. Spectra and GC-MS traces are included in *SI Appendix*. The chemicals were dissolved in DMSO or ethanol and diluted further into working concentrations before experiments.

Heterologous Expression of ORs. A HEK 293T-derived Hana3A cell line was grown in Minimum Essential Medium (HyClone) containing 10% (vol/vol) FBS at 37 °C with 5% (vol/vol) CO $_2$. Lipofectamine 2000 (Invitrogen) was used for transfection. Luciferase assays were performed as previously described. After 18–24 h, OR, the accessory OR protein, mRTP15, and constructs for firefly luciferase and *Renilla* luciferase expression were transfected into cells. Twenty-four hours after transfection, the cells were stimulated with odorants [plus 30 μM Cu $^{2+}$ ions when the ligands were MTMT-, bis(methylthiomethyl) disulfide, and dimethyl sulfide-dissolved in CD293 (Invitrogen)]. We used the Dual-Glo Luciferase Assay System (Promega) and followed the manufacturer's instructions for measuring chemiluminescence.

Statistical Analyses. One-way ANOVA or an unpaired Student's *t* test was used to compare the 95% confidence interval logEC $_{50}$ values among isotopomers for each receptor/odorant pair in Figs. 3 and 4. The level of significance was $*P < 0.05$. An *F* test was used to compare the best-fit values of EC $_{50}$, Hill slope, and top of the dose–response curves between the original hydrogenated odorant and its isotopomers in Figs. 3 and 4 and *SI Appendix*, Fig. S3.2. Bonferroni correction was applied to the *F* tests to account for multiple comparisons. The level of significance was $*P < 0.00076$ before correction and $*P < 0.05$ after correction.

ACKNOWLEDGMENTS. We thank Marshall Newton, Leslie Vosshall, Avery Gilbert, and Andreas Keller for their valuable comments on the manuscript. The authors acknowledge support from the National Science Foundation (Grant CHE-1265679 to E.B. and Grant CHE-1362926 to S.J.); the National Science Foundation Faculty Early Career Development Program (CAREER Grant CHE-0846899 to S.J. and Grant CHE-1213742 to V.S.B.); the Chinese Academy of Sciences for a Visiting Professorship for Senior International Scientists (to E.B.); the Camille Dreyfus Teacher Scholar Award (to S.J.); the Program for Innovative Research Team of Shanghai Municipal Education Commission (H.Z.); the Shanghai Eastern Scholar Program (Grant J50201 to H.Z.); the National Basic Research Program of China (Grant 2012CB910401 to H.Z.); a Computational Materials and Chemical Sciences project under Contract DE-AC02-98CH10886 with the US Department of Energy and supported by its Division of Chemical Sciences, Geosciences, and Biosciences, Office of Basic Energy Sciences (to M.Z.E.); and the NIH (Grants DC005782 and DC012095 to H.M.).

- Ogle W (1870) Anosmia, or cases illustrating the physiology and pathology of the sense of smell. *Med Chir Trans* 53:263–290.
- Sell CS (2014) *Chemistry and the Sense of Smell* (Wiley, Hoboken, NJ).
- Moncrieff RW (1967) *The Chemical Senses* (Leonard Hill, London), 3rd Ed.
- Dyson GM (1938) The scientific basis of odor. *Chem Ind* 57(28):647–651.
- Dyson GM (1928) Some aspects of the vibration theory of odor. *Perfumery and Essential Oil Record* 19:456–459.
- Wright RH, Reid C, Evans HGV (1956) Odor and molecular vibration. III. A new theory of olfactory stimulation. *Chem Ind* (37):973–977.
- Wright RH (1977) Odor and molecular vibration: Neural coding of olfactory information. *J Theor Biol* 64(3):473–502.
- Wright RH (1961) Odour and molecular vibration. *Nature* 190(4781):1101–1102.
- Turin L (1996) A spectroscopic mechanism for primary olfactory reception. *Chem Senses* 21(6):773–791.
- Turin L (1997) The nose as spectroscopist. *Chem Ind* (21):866–870.
- Burr C (2002) *The Emperor of Scent: A Story of Perfume, Obsession, and the Last Mystery of the Senses* (Random House, New York).
- Gilbert AN (2003) The emperor's new theory. *Nat Neurosci* 6(4):335.
- Wolf EL (1985) *Principles of Electronic Tunneling Spectroscopy* (Oxford Univ Press, New York).
- Gane S, et al. (2013) Molecular vibration-sensing component in human olfaction. *PLoS ONE* 8(1):e55780.
- Duan X, et al. (2012) Crucial role of copper in detection of metal-coordinating odorants. *Proc Natl Acad Sci USA* 109(9):3492–3497.
- Sekharan S, et al. (2014) QM/MM model of the mouse olfactory receptor MOR244-3 validated by site-directed mutagenesis experiments. *Biophys J* 107(5):L5–L8.
- Franco MI, Turin L, Merzhin A, Skoulakis EMC (2011) Reply to Hettinger: Olfaction is a physical and a chemical sense in *Drosophila*. *Proc Natl Acad Sci USA* 108(31):E350 (lett).
- Hettinger TP (2011) Olfaction is a chemical sense, not a spectral sense. *Proc Natl Acad Sci USA* 108(31):E349 (lett).
- Wade D (1999) Deuterium isotope effects on noncovalent interactions between molecules. *Chem Biol Interact* 117(3):191–217.
- Schramm VL (2007) Binding isotope effects: Boon and bane. *Curr Opin Chem Biol* 11(5):529–536.
- Pauling L, Delbrück M (1940) The nature of the intermolecular forces operative in biological processes. *Science* 92(2378):77–79.

22. Turin L (2005) Rational odorant design. *Chemistry and Technology of Flavors and Fragrances*, ed Rowe DJ (Blackwell, Oxford), pp 261–273.
23. Rizvanovic A, Amundin M, Laska M (2013) Olfactory discrimination ability of Asian elephants (*Elephas maximus*) for structurally related odorants. *Chem Senses* 38(2): 107–118.
24. Laska M, Shepherd GM (2007) Olfactory discrimination ability of CD-1 mice for a large array of enantiomers. *Neuroscience* 144(1):295–301.
25. Rubin BD, Katz LC (2001) Spatial coding of enantiomers in the rat olfactory bulb. *Nat Neurosci* 4(4):355–356.
26. Saito H, Chi Q, Zhuang H, Matsunami H, Mainland JD (2009) Odor coding by a Mammalian receptor repertoire. *Sci Signal* 2(60):ra9.
27. Shirasu M, et al. (2014) Olfactory receptor and neural pathway responsible for highly selective sensing of musk odors. *Neuron* 81(1):165–178.
28. Axel R (2005) Scents and sensibility: A molecular logic of olfactory perception (Nobel lecture). *Angew Chem Int Ed Engl* 44(38):6110–6127.
29. Buck LB (2005) Unraveling the sense of smell (Nobel lecture). *Angew Chem Int Ed Engl* 44(38):6128–6140.
30. Haffenden LJW, Yaylayan VA, Fortin J (2001) Investigation of vibrational theory of olfaction with variously labelled benzaldehydes. *Food Chem* 73(1):67–72.
31. Keller A, Vosshall LB (2004) A psychophysical test of the vibration theory of olfaction. *Nat Neurosci* 7(4):337–338.
32. Nagashima A, Touhara K (2010) Enzymatic conversion of odorants in nasal mucus affects olfactory glomerular activation patterns and odor perception. *J Neurosci* 30(48):16391–16398.
33. Raju VS, Sharma PK, Banerji KK (2000) Kinetics and mechanism of the oxidation of substituted benzaldehydes by benzyltrimethylammonium chlorobromate. *J Org Chem* 65(11):3322–3325.
34. Seok WK, Meyer TJ (2005) Mechanism of oxidation of benzaldehyde by polypyridyl oxo complexes of Ru(IV). *Inorg Chem* 44(11):3931–3941.
35. Turin L, Yoshii F (2003) Structure-odor relations: A modern perspective. *Handbook of Olfaction and Gustation*, ed Doty RL (Marcel Dekker, New York), pp 275–294.
36. Franco MI, Turin L, Mershin A, Skoulakis EM (2011) Molecular vibration-sensing component in *Drosophila melanogaster* olfaction. *Proc Natl Acad Sci USA* 108(9): 3797–3802.
37. Bittner ER, Madalan A, Czader A, Roman G (2012) Quantum origins of molecular recognition and olfaction in *Drosophila*. *J Chem Phys* 137(22):22A551.
38. Gronenberg W, et al. (2014) Honeybees (*Apis mellifera*) learn to discriminate the smell of organic compounds from their respective deuterated isotopomers. *Proc Biol Sci* 281(1778):20133089.
39. Doolittle RE, Beroza M, Keiser I, Schneider EL (1968) Deuteration of the melon fly attractant, cue-lure, and its effect on olfactory response and infra-red absorption. *J Insect Physiol* 14(12):1697–1712.
40. Blum MS, Doolittle RE, Beroza M (1971) Alarm pheromones: Utilization in evaluation of olfactory theories. *J Insect Physiol* 17(12):2351–2361.
41. Barker RJ, Berdel RL, Waller GD (1973) The molecular basis for scent discrimination: Response to nitrobenzene-d5 of honey bees (*Apis mellifera* L.) conditioned with nitrobenzene. *Experientia* 29(4):418–419.
42. Klika KD (2013) The potential of ¹³C isotopomers as a test for the vibrational theory of olfactory sense recognition. *ISRN Org Chem* 2013:515810.
43. Brookes JC, Hartoutsiou F, Horsfield AP, Stoneham AM (2007) Could humans recognize odor by phonon assisted tunneling? *Phys Rev Lett* 98(3):038101.
44. Brookes JC (2010) Science is perception: What can our sense of smell tell us about ourselves and the world around us? *Philos Trans A Math Phys Eng Sci* 368(1924): 3491–3502.
45. Brookes JC (2011) Olfaction: The physics of how smell works? *Contemp Phys* 52(5): 385–402.
46. Brookes JC, Horsfield AP, Stoneham AM (2012) The swipe card model of odorant recognition. *Sensors (Basel)* 12(11):15709–15749.
47. Solov'yov IA, Chang PY, Schulten K (2012) Vibrationally assisted electron transfer mechanism of olfaction: Myth or reality? *Phys Chem Chem Phys* 14(40):13861–13871.
48. Winkler JR, Gray HB (2014) Long-range electron tunneling. *J Am Chem Soc* 136(8): 2930–2939.
49. Maegawa T, et al. (2008) Mild and efficient H/D exchange of alkanes based on C-H activation catalyzed by rhodium on charcoal. *Angew Chem Int Ed Engl* 47(29): 5394–5397.
50. Harding KE, May LM, Dick KF (1975) Selective oxidation of allylic alcohols with chromic acid. *J Org Chem* 40(11):1664–1665.
51. Wesslen B (1968) Aldol reactions of formaldehyde in non-aqueous media. 4. Mechanism of acid-catalyzed reaction of 2-butanone with formaldehyde. *Acta Chem Scand* 22(7):2085–2110.
52. Saito H, Kubota M, Roberts RW, Chi Q, Matsunami H (2004) RTP family members induce functional expression of mammalian odorant receptors. *Cell* 119(5):679–691.
53. Zhuang H, Matsunami H (2008) Evaluating cell-surface expression and measuring activation of mammalian odorant receptors in heterologous cells. *Nat Protoc* 3(9): 1402–1413.
54. McClintock TS, et al. (2014) In vivo identification of eugenol-responsive and muscone-responsive mouse odorant receptors. *J Neurosci* 34(47):15669–15678.
55. Nara K, Saraiva LR, Ye X, Buck LB (2011) A large-scale analysis of odor coding in the olfactory epithelium. *J Neurosci* 31(25):9179–9191.
56. Morton TH (2000) Archiving odors. *Of Molecules and Mind*, eds Bhushan N, Rosenfeld S (Oxford Univ Press, Oxford), pp 251–272.
57. Schilling B, Kaiser R, Natsch A, Gautschi M (2010) Investigation of odors in the fragrance industry. *Chemoecology* 20:135–147.
58. Mozell MM (1970) Evidence for a chromatographic model of olfaction. *J Gen Physiol* 56(1):46–63.
59. Hahn I, Scherer PW, Mozell MM (1994) A mass transport model of olfaction. *J Theor Biol* 167(2):115–128.
60. Wilkes FJ, Laing DG, Hutchinson I, Jinks AL, Monteleone E (2009) Temporal processing of olfactory stimuli during retronasal perception. *Behav Brain Res* 200(1):68–75.
61. Turowski M, et al. (2003) Deuterium isotope effects on hydrophobic interactions: The importance of dispersion interactions in the hydrophobic phase. *J Am Chem Soc* 125(45):13836–13849.
62. Renz M, Meunier B (1999) 100 years of Baeyer-Villiger oxidations. *European J Org Chem* 1999(4):737–750.
63. Zhuo X, et al. (1999) Biotransformation of coumarin by rodent and human cytochromes P-450: Metabolic basis of tissue-selective toxicity in olfactory mucosa of rats and mice. *J Pharmacol Exp Ther* 288(2):463–471.
64. Thiebaud N, et al. (2013) Odorant metabolism catalyzed by olfactory mucosal enzymes influences peripheral olfactory responses in rats. *PLoS ONE* 8(3):e59547.
65. Sharma R, et al. (2012) Deuterium isotope effects on drug pharmacokinetics. I. System-dependent effects of specific deuteration with aldehyde oxidase cleared drugs. *Drug Metab Dispos* 40(3):625–634.
66. Leggett AJ, et al. (1987) Dynamics of the dissipative two-state system. *Rev Mod Phys* 59(1):1–85.
67. Jortner J (1976) Temperature-dependent activation-energy for electron-transfer between biological molecules. *J Chem Phys* 64(12):4860–4867.
68. Marcus RA (1965) On theory of electron-transfer reactions. 6. Unified treatment for homogeneous and electrode reactions. *J Chem Phys* 43(2):679–701.
69. Moser CC, Keske JM, Warncke K, Farid RS, Dutton PL (1992) Nature of biological electron transfer. *Nature* 355(6363):796–802.
70. Gray HB, Winkler JR (1996) Electron transfer in proteins. *Annu Rev Biochem* 65: 537–561.
71. Jia Y, et al. (1993) Primary charge separation in mutant reaction centers of *Rhodospirillum rubrum*. *J Phys Chem* 97(50):13180–13191.
72. Wang H, et al. (2007) Protein dynamics control the kinetics of initial electron transfer in photosynthesis. *Science* 316(5825):747–750.
73. Ulstrup J, Jortner J (1975) Effect of intramolecular quantum modes on free-energy relationships for electron-transfer reactions. *J Chem Phys* 63(10):4358–4368.
74. Jang S, Newton MD (2006) Closed-form expressions of quantum electron transfer rate based on the stationary-phase approximation. *J Phys Chem B* 110(38):18996–19003.
75. Jortner J (1999) *Electron Transfer—From Isolated Molecules to Biomolecules*, ed Bixon M (Wiley, Hoboken, NJ), Vol 106.
76. Venkataraman L, Klare JE, Nuckolls C, Hybertsen MS, Steigerwald ML (2006) Dependence of single-molecule junction conductance on molecular conformation. *Nature* 442(7105):904–907.
77. Medvedev ES, Stuchebrukhov AA (1997) Inelastic tunneling in long-distance biological electron transfer reactions. *J Chem Phys* 107(10):3821–3831.
78. Jang S, Newton MD (2005) Theory of torsional non-Condon electron transfer: A generalized spin-boson Hamiltonian and its nonadiabatic limit solution. *J Chem Phys* 122(2):024501.
79. Oka Y, et al. (2006) Odorant receptor map in the mouse olfactory bulb: In vivo sensitivity and specificity of receptor-defined glomeruli. *Neuron* 52(5):857–869.
80. Keller A, Zhuang H, Chi Q, Vosshall LB, Matsunami H (2007) Genetic variation in a human odorant receptor alters odour perception. *Nature* 449(7161):468–472.
81. Menashe I, et al. (2007) Genetic elucidation of human hyperosmia to isovaleric acid. *PLoS Biol* 5(11):e284.
82. Baud O, et al. (2011) The mouse eugenol odorant receptor: Structural and functional plasticity of a broadly tuned odorant binding pocket. *Biochemistry* 50(5):843–853.
83. Takane SY, Mitchell JB (2004) A structure-odor relationship study using EVA descriptors and hierarchical clustering. *Org Biomol Chem* 2(22):3250–3255.
84. Gabler S, Soelster J, Hussain T, Sachse S, Schmuker M (2013) Physicochemical vs. vibrational descriptors for prediction of odor receptor responses. *Mol Inform* 32(9–10): 855–865.
85. Triller A, et al. (2008) Odorant-receptor interactions and odor percept: A chemical perspective. *Chem Biodivers* 5(6):862–886.

Supporting Information

Implausibility of the vibrational theory of olfaction

Eric Block, Seogjoo Jang, Hiroaki Matsunami, Sivakumar Sekharan, Bérénice Dethier, Mehmed Z. Ertem, Sivaji Gundala, Yi Pan, Shengju Li, Zhen Li, Stephene N. Lodge, Mehmet Ozbil, Huihong Jiang, Sonia Flores Penalba, Victor S. Batista and Hanyi Zhuang

Table of Contents

Part 1. Detailed theoretical analysis of the vibrational theory of olfaction [Seogjoo Jang]

Figure S1.1

Figure S1.2

Figure S1.3

Part 2. Synthesis and characterization of deuterated ligands [Eric Block, Bérénice Dethier, Sivaji Gundala, Stephene N. Lodge, Sonia Flores Penalba]

Figure S2.1 Cyclopentadecanol-d₂₉ (**2**-d₂₉) GC-MS.

Figure S2.2 Cyclopentadecanol-d₂₉ (**2**-d₂₉) IR spectrum.

Figure S2.3 Cyclopentadecane-d₃₀ (**3**-d₃₀) GC-MS.

Figure S2.4 Cyclopentadecane-d₃₀ (**3**-d₃₀) IR spectrum.

Figure S2.5 Cyclopentadecanone-d₂₈ (**1**-d₂₈) GC-MS.

Figure S2.6 Cyclopentadecanone-d₂₈ (**1**-d₂₈) ¹H NMR spectrum.

Figure S2.7 Commercial cyclopentadecanone (**1**) ¹H NMR spectrum.

Figure S2.8 Cyclopentadecanone-d₂₈ (**1**-d₂₈) IR spectrum.

Figure S2.9 Cyclopentadecanone (commercial; **1**) IR spectrum.

Figure S2.10 Cyclopentadecanone-2,2,15,15-d₄ (**1**-d₄) ¹H (top) and ¹³C (bottom) NMR spectra.

Figure S2.11 Cyclopentadecanone-2,2,15,15-d₄ (**1**-d₄) IR spectrum.

Figure S2.12 *d,l*-3-Methylcyclopentadecanone-d₃₀ (muscone-d₃₀; **4**-d₃₀) GC-MS.

Figure S2.13 *d,l*-3-Methylcyclopentadecanone (muscone; **4**) GC-MS.

Figure S2.14 *d,l*-3-Methylcyclopentadecanone (muscone; **4**; *top*) and *d,l*-3-methylcyclopentadecanone-d₃₀ (muscone-d₃₀; **4**-d₃₀; *bottom*) ¹H NMR spectra.

Figure S2.15 Chloromethyl methyl sulfide-d₅.

Figure S2.16 (Methylthio)methanethiol-d₅.

Figure S2.17 2,4,5,7-Tetrathiaoctane-d₁₀ (**9**-d₁₀).

Part 3. Screening for human cyclopentadecanone receptor and the response of various ORs to isotopomers [Hiroaki Matsunami, Huihong Jiang, Shengju Li, Zhen Li, Yi Pan, Hanyi Zhuang]

Figure S3.1. Screening for human ORs for all four isotopomers of cyclopentadecanone done using luciferase assays of 330 unique human odorant receptors.

Figure S3.2. Dose-response curves of A) mouse and B) human ORs to various isotopomeric groups of compounds.

Figure S3.3. Response of human OR5AN1 to representative musk compounds

Table S3.1. A list of musk and other compounds and their isotopomers used in Figures 2 and S3.2.

Table S3.2. Pairwise comparisons between the dosage response curves for the original odorant and its deuterated or ¹³C isotopomers with an *F* test.

Part 4. QM/MM binding affinity calculations of deuterated and non-deuterated MTMT [Sivakumar Sekharan, Mehmed Z. Ertem, Mehmet Ozbil, Victor S. Batista]

Table S4.1. ONIOM enthalpies and Gibbs free energies in units of Hartrees for the optimized MOR244-3 model in complex with deuterated and non-deuterated MTMT.

Table S4.2. Gibbs free energies in units of Hartrees for undeuterated and deuterated ligand as itself and bound in receptor active site with associated deuterium isotope effects.

Supporting Information: Part 1

In this part of the Supporting Information, we provide more detailed theoretical analysis of the vibrational theory of olfaction (VTO) by Brookes *et al.*,¹ and present results of model calculation showing that inclusion of non-odorant quantum vibrational modes could easily mask the effect of odorant vibrations. The Hamiltonian proposed by Brookes *et al.*¹ is a form of well-known spin-boson Hamiltonian,² which can be expressed as¹⁴

$$H = H_e + H_c + H_b + H_{eb} , \quad (1)$$

where H_e is the electronic Hamiltonian representing the donor and the acceptor states, H_c is the coupling between them, H_b is the bath Hamiltonian, and H_{eb} is the electron-bath coupling Hamiltonian. The bath here refers to all other degrees of freedom except for the electronic states of the donor and the acceptor. The detailed forms of the above Hamiltonian components are as follows:

$$H_e = E_D |D\rangle\langle D| + E_A |A\rangle\langle A| , \quad (2)$$

$$H_c = J(|D\rangle\langle A| + |A\rangle\langle D|) , \quad (3)$$

$$\begin{aligned} H_b &= \sum_n \hbar\omega_n (b_n^\dagger b_n + \frac{1}{2}) + \hbar\omega_o (b_o^\dagger b_o + \frac{1}{2}) \\ &= H_b^0 + H_b^1 , \end{aligned} \quad (4)$$

$$\begin{aligned} H_{eb} &= \sum_n \hbar\omega_n (b_n + b_n^\dagger)(g_{nD}|D\rangle\langle D| + g_{nA}|A\rangle\langle A|) \\ &\quad + \hbar\omega_o (b_o + b_o^\dagger)(g_{oD}|D\rangle\langle D| + g_{oA}|A\rangle\langle A|) \\ &= H_{eb}^0 + H_{eb}^1 . \end{aligned} \quad (5)$$

In the above expressions, $|D\rangle$ represents the quantum mechanical state where the electron (or hole) is in the donor, and $|A\rangle$ the state where electron (or hole) is in the acceptor. E_D and E_A are their respective energies and J is the electronic coupling between them. All the bath degrees of freedom including the odorant are approximated as harmonic oscillators. We denote all the bath degrees of freedom except for the odorant oscillator with H_b^0 and the odorant oscillator with H_b^1 . For each bath oscillator in H_b^0 , the frequency is given by ω_n , and the raising and lowering operators are given by b_n^\dagger and b_n . The frequency of the odorant oscillator is ω_o , and the raising and lowering operators of the odorant oscillator are b_o^\dagger and b_o . The above Hamiltonian can easily be extended to the case with many vibrational modes,³ which does not affect the main conclusion drawn here.

For the model Hamiltonian described above, application of Fermi's golden rule leads to the following integral expression for the rate:

$$k = \frac{J^2}{\hbar^2} \int_{-\infty}^{\infty} dt e^{-it\Delta G^0/\hbar - (\mathcal{K}_b(0) - \mathcal{K}_b(t)) - (\mathcal{K}_o(0) - \mathcal{K}_o(t))} , \quad (6)$$

where ΔG^0 is the Gibbs free energy for the above model

defined as

$$\begin{aligned} \Delta G^0 &= E_A - E_D - \sum_n \hbar\omega_n (g_{nA}^2 - g_{nD}^2) \\ &\quad - \hbar\omega_o (g_{oA}^2 - g_{oD}^2) , \end{aligned} \quad (7)$$

$\mathcal{K}_b(t)$ is the bath correlation function defined as

$$\mathcal{K}_b(t) = \sum_n S_n \left(\coth\left(\frac{\beta\hbar\omega_n}{2}\right) \cos(\omega_n t) - i \sin(\omega_n t) \right) , \quad (8)$$

with the Huang-Rhys factor for each bath mode $S_n = (g_{nD} - g_{nA})^2$, and $\mathcal{K}_o(t)$ is the correlation function of the odorant mode defined as

$$\mathcal{K}_o(t) = S_o \left(\coth\left(\frac{\beta\hbar\omega_o}{2}\right) \cos(\omega_o t) - i \sin(\omega_o t) \right) , \quad (9)$$

with the Huang-Rhys factor for the odorant oscillator $S_o = (g_{oD} - g_{oA})^2$.

If $S_o = 0$ and under the assumption that all the bath modes (except for the odorant) behave classically, Eq. (6) reduces⁴ to the following Marcus formula:^{5,6}

$$k_M = \frac{2\pi}{\hbar} \frac{J^2}{\sqrt{4\pi k_B T \lambda}} \exp \left\{ -\frac{(\Delta G^0 + \lambda)^2}{4\lambda k_B T} \right\} , \quad (10)$$

where

$$\lambda = \sum_n S_n \hbar\omega_n . \quad (11)$$

For finite but small value of S_o , Eq. (6) reduces to the following one quantum version of the Marcus-Jortner formula:⁷

$$k_{MJ} = \frac{2\pi}{\hbar} \frac{J^2 e^{-S_o} S_o}{\sqrt{4\pi k_B T \lambda}} \exp \left\{ -\frac{(\Delta G^0 + \hbar\omega_o + \lambda)^2}{4\lambda k_B T} \right\} . \quad (12)$$

Brookes *et al.*¹ define two transfer times τ_0 and τ_1 , which are ET transfer times in the absence and presence of odorant oscillator, respectively. These are identified as inverses of the ET rates as follows: $1/\tau_0 = k_M$ and $1/\tau_1 = k_{MJ}$. Assuming that the likelihood of detection depends on relative transfer times, they use the following ratio as the measure of detection sensitivity:

$$\frac{\tau_0}{\tau_1} = S_o \exp \left\{ -S_o - \frac{2\hbar\omega_o(\Delta G^0 + \lambda) + \hbar^2\omega_o^2}{4k_B T \lambda} \right\} . \quad (13)$$

Then, following Turin's suggestion,⁸ Brookes *et al.*¹ assume that the optimum energetic condition occurs¹⁵ for $\Delta G^0 = -\hbar\omega_o$. The resulting optimum ratio can be expressed as

$$\left. \frac{\tau_0}{\tau_1} \right|_{opt} = S_o \exp \left\{ -S_o + \frac{\hbar\Omega}{4k_B T} \left(\frac{\hbar\Omega}{\lambda} - 2 \right) \right\} . \quad (14)$$

For this to be large enough, they estimate¹ that the reorganization energy, $\lambda \approx 30$ meV. However, this value is much smaller than typical values of reorganization energy in biological ET processes.^{9–13} Recent assessment of the reorganization energy for the charge transfer in the bacterial reaction center of photosynthesis is in the range of 100 – 300 meV.¹⁰ Even for long range ET reactions in biological environments,^{11–13} the reorganization energy is estimated to be about 1 eV and not less than 700 meV. Thus, the assumption of such a small reorganization energy in the odorant receptor site is unprecedented. However, this may not be a serious issue because resolution of such unrealistic assumption is possible if we recognize the fact that the maximum value for Eq. (13) in fact occurs for $\Delta G^0 = -\hbar\omega_o - \lambda$ and is given by

$$\frac{\tau_0}{\tau_1} \Big|_{max} = S_o \exp \left\{ -S_o + \frac{(\hbar\omega_o)^2}{4\lambda k_B T} \right\}. \quad (15)$$

According to the above expression, the criteria set by Brookes *et al*¹ can be satisfied as long as $\lambda \ll (\hbar\omega_o)^2/(k_B T)$ and $S_o \ll 1$, which in fact allows reasonably large value of λ .

The assumption behind Eqs. (10) and (12) is that all the bath degrees of freedom except for the odorant oscillator can be approximated as classical, for which there is no supporting experimental evidence. If the vibration of odorant molecules is assumed to couple to the ET through charge and induced polarization interaction,¹ there is no reason why the vibrational modes corresponding to metal-ligand bonds (assuming they indeed exist as proposed by Turin) and those of protein residues near the donor or acceptor sites are not coupled to the ET in a similar manner if not more strongly. The implication of this is that the bath spectral density should be extended to include such vibrational frequencies, for which the rate expressions of Eqs. (10) and (12) are no longer valid. Therefore, it is important to analyze the potential influence of quantum effects of other vibrational modes. Before illustrating our point further, let us define the following conventional spectral density of the bath:

$$\mathcal{J}(\omega) = \sum_n \delta(\omega - \omega_n) S_n \omega_n^2. \quad (16)$$

Then, the bath correlation function of Eq. (8) can be expressed as

$$\mathcal{K}_b(t) = \int_0^\infty d\omega \frac{\mathcal{J}(\omega)}{\omega^2} \left(\coth \left(\frac{\beta \hbar \omega}{2} \right) \cos(\omega t) - i \sin(\omega t) \right) \quad (17)$$

We here consider the case where the bath spectral density is given by the following Ohmic form with exponential cutoff:

$$\mathcal{J}(\omega) = \eta \omega e^{-\omega/\omega_c}. \quad (18)$$

For the above spectral density, the reorganization energy is given by $\lambda = \eta \hbar \omega_c$.

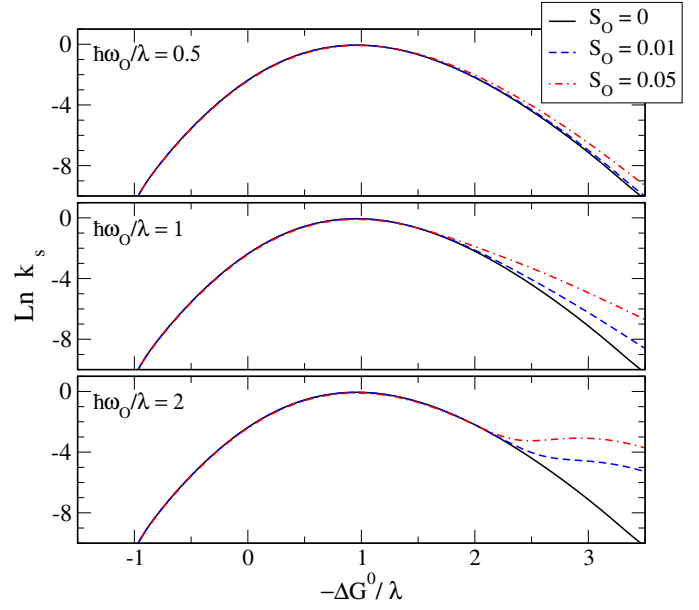


Figure S1.1. Comparison of scaled rate $k_s = k\hbar\sqrt{4\pi k_B T \lambda}/(2\pi J^2)$ for the Ohmic spectral density of Eq. (18) with $\eta = 10$, $\hbar\omega_c/k_B T = 1$. The corresponding ratio of the reorganization energy to temperature is $\lambda/k_B T = 10$.

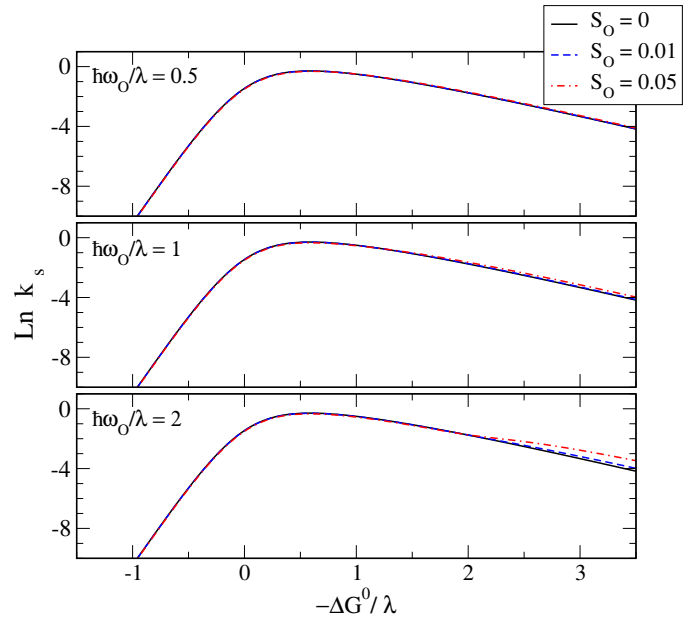


Figure S1.2. Comparison of scaled rate $k_s = k\hbar\sqrt{4\pi k_B T \lambda}/(2\pi J^2)$ for the Ohmic spectral density of Eq. (18) with $\eta = 2$, $\hbar\omega_c/k_B T = 5$. The corresponding ratio of the reorganization energy to temperature is $\lambda/k_B T = 10$.

We have calculated the ET rate given by Eq. (6) directly through numerical Fourier transform for reason-

able value of $\lambda = 10k_B T$ and for different values of η , ω_c , and S_O . The results in Fig. S1.1 correspond to the case where all the bath modes are classical or nearly classical. As implied by Eq. (15), we find the effect of coupling to odorant oscillator becomes significant for $\hbar\omega_o \geq \lambda$. However, even such enhancement becomes obscure for quantum mechanical bath as shown in Fig. S1.2. The cutoff frequency of the bath in this case is five times that of the thermal energy. Thus, assuming 300 K, such cutoff frequency amounts to a vibration of about $1,000 \text{ cm}^{-1}$. Even for this moderate value of the cutoff frequency, Fig. S1.2 shows that the effect of odorant oscillator does not stand out significantly even up to the value of $\omega_o \approx 4,000 \text{ cm}^{-1}$.

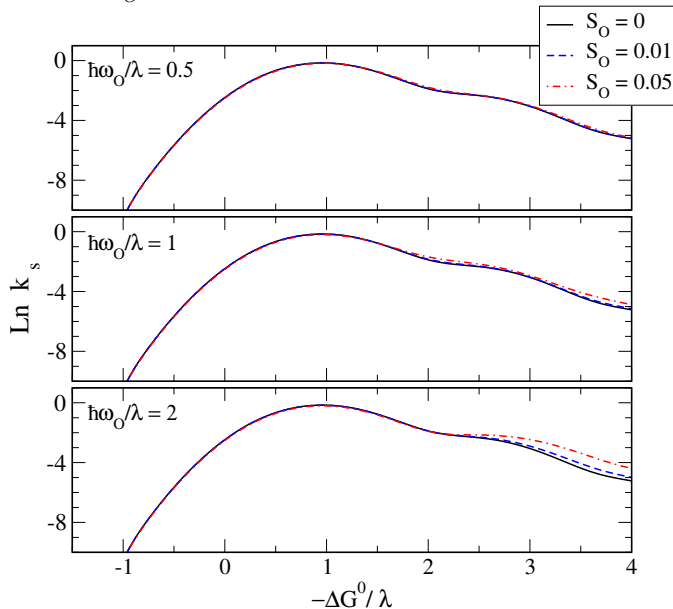


Figure S1.3. Comparison of scaled rate $k_s = k\hbar\sqrt{4\pi k_B T \lambda}/(2\pi J^2)$ for the spectral density of Eq. (19) with $\eta = 10$, $\hbar\omega_c/k_B T = 1$, $S_q = 0.1$, and $\omega_q/\omega_c = 15$. The corresponding ratio of the reorganization energy to temperature is $\lambda/k_B T = 10$.

Actual spectral densities are in general much more complex and, often, there are quantum modes well separated from classical modes. As a simple representation of such case, we considered the following spectral density:

$$\mathcal{J}(\omega) = \eta\omega e^{-\omega/\omega_c} + S_q\omega_q^2\delta(\omega - \omega_q). \quad (19)$$

The total reorganization energy (but without including the effects of the odorant) in this case is given by $\lambda_T = \lambda + S_q\hbar\omega_q$, where λ has been defined below Eq. (18). We have calculated the ET rates for the above spectral density once again by direct numerical calculation of Eq. (6) through Fourier transform. We have chosen $S_q = 0.1$ and $\omega_q/\omega_c = 15$, while keeping all other parameters the same as those for Fig. S1.1. The results shown in Fig. S1.3 demonstrate that the sensitivity observed in Fig. S1.1 has disappeared in this case because of the additional quantum mode in the bath. Any actual spectral density in biological environments is expected to be much more complex than Eq. (19). Detecting the frequency of the odorant through different ETs, as proposed by the VTO, in such environment appears to be much more difficult. In addition, such hypothetical detection efficiency is likely to degrade further due to thermal fluctuations and disorder.

In the main text, Fig. 3 provides the results of τ_0/τ_1 , which is calculated by taking the ratio of the rate for finite value of S_O to that with $S_O = 0$. These results confirm that the proposed mechanism of VTO is effective only for sufficiently large frequency of the odorant oscillator, ω_o , for a given value of reorganization energy. Most importantly, even such enhancement can easily be overridden once quantum vibrational modes in the bath (the donor/acceptor sites or other environments) become active even by modest amount.

The importance of high frequency vibrational modes in the inverted regime of ET, where the proposed mechanism of VTO is active, is a well established fact, in particular, in biological environments. On the other hand, the key assumption of VTO¹ as demonstrated here is that such molecular vibrations of the environment do not contribute to the ET so that the spectral range of the bath is cleared for the detection of odorant frequency only. While such assumption may be reasonable for conventional inelastic tunneling spectroscopy involving metal electrodes as the donor and the acceptor of the electron, it lacks clear justification in biological molecular environments. Moreover, even if the proposed ET involved metal atomic centers and the transferring electron (or hole) were significantly delocalized, the effects of non-odorant molecular environments near the electron (hole) centers would be more important than those of weakly bound odorant molecule.

¹ Brookes JC, Hartoutsiou F, Horsfield AP, & Stoneham, AM (2007) Could humans recognize odor by phonon assisted tunneling? *Phys. Rev. Lett.* 98:038101.

² Leggett AJ, Chakravarty S, Dorsey AT, Fisher MPA, Garg A, & Zwerger W (1987) Dynamics of the dissipative 2-state system. *Rev. Mod. Phys.* 59:1.

³ Solov'yov IA, Chang PY, & Schulten K (2012) Vibrationally assisted electron transfer mechanism of olfaction: myth or reality? *Phys. Chem. Chem. Phys.* 14:13861.

⁴ Jang S & Newton MD (2006) Closed form expressions of quantum electron transfer rate based on the stationary phase approximation. *J. Phys. Chem. B* 110:18996.

- ⁵ Marcus RA (1956) On the theory of oxidation-reduction reactions involving electron transfer. I. *J. Chem. Phys.* 24:966.
- ⁶ Marcus RA (1965) Theory of electron-transfer rates of solvated electrons. *J. Chem. Phys.* 43:679.
- ⁷ Jortner J (1976) Temperature dependent activation energy for electron transfer between biological molecules. *J. Chem. Phys.* 64:4860.
- ⁸ Turin L (1996) A spectroscopic mechanism for primary olfactory reception. *Chem. Senses* 21:773.
- ⁹ Moser CC, Keske JM, Warncke K, Faird RS, & Dutton PL (1992) Nature of biological electron transfer *Nature* 796:355.
- ¹⁰ LeBard DN, Matyushov DV (2009) Energetics of Bacterial Photosynthesis. *J. Phys. Chem. B* 113:12424.
- ¹¹ Gray HB and Winkler JR (1996) Electron transfer in proteins *Annu. Rev. Biochem.* 65:537.
- ¹² Gray HB and Winkler JR (2005) Long-range electron transfer *Proc. Natl. Acad. Sci., USA* 102:3534.
- ¹³ Skourtis SS, Balabin IA, Kawatsu T, & Beratan DN (2005) Protein dynamics and electron transfer: Electronic decoherence and non-Condon effects *Proc. Natl. Acad. Sci., USA* 102:3552.
- ¹⁴ We here adopt a different notation than that used by Brookes *et al.*
- ¹⁵ In fact, the energy difference $E_A - E_D$ rather than the free energy of reaction is used in Ref. 1

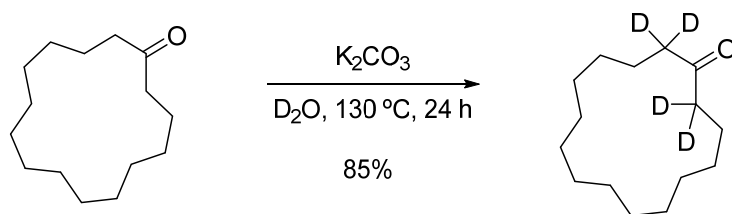
Supporting Information. Part 2. Synthesis and Characterization of Deuterated Ligands

Cyclopentadecanol-d₂₉ (2-d₂₉). Cyclopentadecanone (**1**; 98%; 1 g, 4.46 mmol), rhodium on carbon (200 mg), cyclohexane (0.8 mL) and D₂O (27 mL) was stirred in a sealed tube under H₂ atmosphere at 150 °C during 15 h (48). After filtration of the rhodium on Celite, the mixture was diluted in saturated aqueous NH₄Cl and extracted with CH₂Cl₂ (×3). The organic layer was dried and concentrated. GC-MS analysis showed the presence of 10:10:1 cyclopentadecanone:cyclopentadecanol:cyclopentadecane (**1:2:3**; 1.2 g; 91% yield calculated for alcohol **2**). The material was then stirred without further purification in a sealed tube with fresh D₂O (27 mL), cyclohexane (0.8 mL) and rhodium on carbon (200 mg) under H₂ atmosphere at 150 °C during 15 h. After dilution in saturated aqueous NH₄Cl, the products are extracted by CH₂Cl₂. The organic layer was dried, concentrated, and analyzed by GC-MS, revealing a mixture of cyclopentadecanone-d₂₈ (**1-d₂₈**; 2%), cyclopentadecanol-d₂₉ (**2-d₂₉**; 94%) and cyclopentadecane-d₃₀ (**3-d₃₀**; 4%). The mixture was purified by column chromatography (hexanes:Et₂O, 10:1), affording cyclopentadecanol-d₂₉ (**2-d₂₉**) as a colorless solid (332 mg, 30% yield), mp 80-81 °C (compare mp **2**, 79-80 °C), with an overall deuterium content of 98.5% by GC-MS; *m/z* 253 (M⁺, 1%), *m/z* 236 (M⁺-DHO, 100%) (Fig. S2.1), IR 3279 (br, OH), 2992 (w, residual C–H), 2195, 2097 (C–D) (Fig. S2.2), ¹H NMR (400 MHz, CDCl₃) δ 1.27 (d, *J* = 8.4 Hz); and cyclopentadecane-d₃₀ (**3-d₃₀**), a colorless solid (87 mg, 8% yield), mp 52-55 °C (compare **3**, mp 60-63 °C), 98% deuterated by GC-MC, *m/z* 240 (Fig. S2.3), IR 2918, 2851 (w, residual C–H), 2194, 2097 (s, C–D) (Fig. S2.4); ¹H NMR (400 MHz, CDCl₃) δ 1.26; ¹³C NMR (100 MHz, CDCl₃) δ 25.97, 25.78, 25.59, 25.41, 25.22.

Cyclopentadecanone-d₂₈ (1-d₂₈). Cyclopentadecanol-d₂₉ (**2-d₂₉**; 120 mg, 0.468 mmol) was dissolved in 2:1 acetone:H₂O (2:1; 6 mL). Then, a solution of K₂Cr₂O₇ (65 mg/mL; 8.8 mL, 0.656 mmol, 1.4 eq) in aqueous H₂SO₄ (12.5% v/v) was added dropwise to the mixture with stirring (49). The mixture was stirred at RT for 3 h, until a dark green coloration appeared. The mixture was extracted by hexanes (×3). The combined organic layers were dried (MgSO₄) and concentrated in vacuo affording cyclopentadecanone-d₂₈ (**1-d₂₈**), a colorless solid (91 mg; 77 % yield) containing 98.9% deuterium as indicated by GC-MS *m/z* 252 (Fig. S2.5). Recrystallization [H₂O/MeOH (1:1)] gave colorless crystals, mp 61-62 °C (compare **1**, mp 62-63 °C); weak ¹H NMR (400 MHz, CDCl₃) δ 2.38 (d, *J* = 10.2 Hz, 5H), and 1.25 (s, 9H); a peak due to water at

1.56 overlapping a third peak (Fig. S2.6). Commercial **1** showed ^1H NMR (400 MHz, CDCl_3) δ 2.41 (t, $J = 6.7$ Hz, 1H), 1.73–1.56 (m, 1H), 1.31 (dd, $J = 20.5, 6.9$ Hz, 5H), (Fig. S2.7), ^{13}C NMR (100 MHz, CDCl_3) δ 42.30, 27.77, 26.96, 26.91, 26.62, 26.48, 23.65, and GC-MS m/z 224. For **1-d**₂₈, IR 2892 (w, residual C-H), 2196, 2098 (s, C-D), 1702 (s, C=O) cm^{-1} (Fig. S2.8) while for commercial **1**, IR (neat): 2923, 2853 (C-H), 1707 (s, C=O) cm^{-1} (Fig. S2.9).

Sham samples of 1, 2 and 3. The same procedure as above for deuteration of **1** was followed except that D_2O was replaced by H_2O . Isolated yields: **1** (350 mg, 35%), mp 58-60 °C; **2** (130 mg, 13%), mp 76-78 °C; **3** (15 mg, 2%), mp 47-49 °C. For **1**: ^1H NMR (400 MHz, CDCl_3 , ppm) δ : 2.40 (t, $J = 7.0$ Hz, 4 H), 1.63 (t, $J = 7.0$ Hz, 4 H), 1.30 (d, $J = 8.0$ Hz, 20 H); ^{13}C NMR (100 MHz, CDCl_3 , ppm) δ : 212.6, 42.1, 27.6, 26.8, 26.7, 26.4, 26.3, 23.4. For **2**: ^1H NMR (400 MHz, CDCl_3 , ppm) δ : 3.73 (t, $J = 6.1$ Hz, 1 H), 1.62-1.53 (m, 2 H), 1.51-1.43 (m, 2 H), 1.42-1.24 (m, 24 H) (-OH not observed); ^{13}C NMR (100 MHz, CDCl_3 , ppm) δ : 70.6, 35.3, 27.1, 26.9, 26.8, 26.7, 26.7, 23.2. For **3**: ^1H NMR (400 MHz, CDCl_3 , ppm) δ : 1.33 (s, 30 H). ^{13}C NMR (100 MHz, CDCl_3 , ppm) δ : 26.9.



Cyclopentadecanone-2,2,15,15-d₄ (1-d₄). A modification of a published procedure (50) described for 2-butanone was used. A mixture of D_2O (9 mL) and **1** (1 g, 4.46 mmol) in the presence of a catalytic amount of K_2CO_3 was refluxed at 130 °C in a sealed tube for 24 h. The reaction mixture was cooled to rt, diluted with saturated aqueous NH_4Cl and extracted (CH_2Cl_2 , $\times 3$). The organic layers were combined, dried (Na_2SO_4) and concentrated in vacuo. The residue was redissolved in fresh D_2O (9 mL), catalytic K_2CO_3 was added and the mixture was stirred in a sealed tube at 130 °C for another 24 h. This process was repeated two more times until an aliquot analysed by GC-MS showed complete deuteration at the desired positions. The crude mixture was purified by column chromatography (eluent: 15:1 hexanes: Et_2O). The title compound **1-d₄** was isolated as a colorless solid (813 mg, 85% yield), mp 54-56 °C; ^1H NMR (400 MHz, CDCl_3 , ppm) δ : 2.39 (d, $J = 8$ Hz, 0.18 H) 1.62 (t, $J = 6.9$ Hz, 4 H), 1.29 (s, 20 H) and ^{13}C NMR (100 MHz, CDCl_3 , ppm) δ : 212.8, 41.4 (t, $^1J_{\text{CD}} = 19.3$ Hz), 27.5, 26.8, 26.7, 26.5, 26.3, 23.3 (Fig. S2.10); IR shows 2854 (C-H), 2160, 2024, 1977 (w, all C-D), 1702 (C=O) cm^{-1} (Fig. S2.11);

GC-MS indicates 93.7% of the maximum possible α -deuteration (m/z 228; M^+). This sample, as described above obtained by chromatography using commercial hexanes, shows a trace ^1H NMR peak at δ 0.8, typical of impurity residues seen with commercial hexanes.

Cyclopentadecanone-3,3,4,4,5,5,6,6,7,7,8,8,9,9,10,10,11,11,12,12,13,13,14,14- d_{24} (1- d_{24}). A mixture of H_2O (9 mL) and cyclopentadecanone- d_{28} (1- d_{28} ; 300 mg, 1.19 mmol) with catalytic K_2CO_3 was refluxed at 130 °C in a sealed tube for 24 h. The reaction mixture was cooled to rt, diluted with saturated aqueous NH_4Cl and extracted (CH_2Cl_2 , $\times 3$). The combined organic layers were combined and the volatiles removed. The residue was then re-dissolved in fresh H_2O , catalytic K_2CO_3 was added and the mixture was stirred in a sealed tube at 130 °C for another 24 h. This process was repeated two more times until an aliquot analysed by GC-MS showed complete D-H exchange at the desired positions. The crude mixture was purified by column chromatography (pentane: Et_2O ; 20:1). Product 1- d_{24} was isolated as a colorless solid (60 mg; 40% yield), mp 54-56 °C, showing 88.3% deuteration (expected for d_{24} , 85.7%), in which all hydrogens *except* the four α -hydrogen atoms are replaced with deuteriums; GC-MS m/z 247 ($M-d_{23}$), 248 ($M-d_{24}$), 249 ($M-d_{25}$), 250 ($M-d_{26}$); ^1H NMR (400 MHz, CDCl_3) δ 2.46–2.32 (m, peak area 4), 1.60 (overlap with water), 1.27 (d, $J = 12.4$ Hz, peak area 3 of possible area 24, so 88% deuterated in non- α positions).

***d,l*-3-Methylcyclopentadecanone- d_{30} (muscone- d_{30} ; 4- d_{30}).** A mixture of muscone (**4**; 220 μL , 202.0 mg, 0.8 mmol), rhodium on carbon (40 mg), cyclohexane (160 μL) and D_2O (5.5 mL) was stirred in a sealed tube under an atmosphere of H_2 at 150 °C during 18 h. After removal of the rhodium/C by filtration through Celite, the mixture was diluted with saturated aqueous NH_4Cl (12.0 mL) and extracted with CH_2Cl_2 . (3 \times 8.0 mL). The organic layers were dried (MgSO_4) and concentrated. GC-MS analysis showed the presence of deuterated muscone (50%), a diastereomeric mixture of deuterated *cis/trans*-3-methylcyclopentadecanol (**5**; 49%) and deuterated methylcyclopentadecane (1%). The material was then stirred without further purification in a sealed tube with fresh D_2O (5.5 mL), cyclohexane (160.0 μL) and rhodium/carbon (40.0 mg) under H_2 atmosphere at 150 °C during 18 h. After dilution with saturated aqueous NH_4Cl (12.0 mL), the products were extracted by CH_2Cl_2 (3 \times 8.0 mL). The organic layers were dried (MgSO_4) and concentrated giving a colorless oil, which was analyzed by GC-MS. The mixture containing diastereomers of deuterated 3-methylcyclopentadecanol (**5**; 85%), muscone- d_{30} (**4- d_{30}** ; 10%), and methylcyclopentadecane- d_{30} (5%), as indicated by GC-MS analysis, was dissolved in

acetone:H₂O (6 mL; 2:1 ratio). A solution of K₂Cr₂O₇ (65 mg/mL) in H₂O/H₂SO₄ (6 mL; 12.5 % v/v) was then added dropwise to the mixture. The flask was stirred at 45 °C for 2 h, until the reaction mixture became dark green. After cooling to RT, the mixture was extracted by hexanes (3 x 8.0 mL). The combined organic layers are dried (MgSO₄) and evaporated under reduced pressure. Muscone-d₃₀, **4-d₃₀**, is obtained as a colorless oil (90 mg; 42% yield) after column chromatography (10:1 hexanes:Et₂O); 96.7% deuterated according to GC-MS analysis, *m/z* 268 (Fig. S2.12; compare *m/z* 238 for muscone **4**, Fig. S2.13); IR (neat) 2197, 2099 (C–D), 1704 (C=O) cm⁻¹ which can be compared with the IR (neat) 2925, 2856 (C–H), 1710 (C=O) cm⁻¹ for undeuterated **4** (Fig. 2)]; NMR similar to, but much weaker, than that of undeuterated **4** (Fig. S2.14).

Chloromethyl methyl sulfide-d₅. Dimethyl sulfoxide-d₆ (25.0 g, 0.3 mol) was dissolved in CH₂Cl₂ (20 mL) and was slowly added to a heated solution of thionyl chloride (23.7 mL, 0.33 mmol, 1.1 eq) in CH₂Cl₂ (60 mL). The reaction mixture was stored overnight at room temperature and distilled to give the title compound as a light yellow liquid (30 g, 98%), bp 104-106 °C ; ¹³C-NMR (100 MHz, CDCl₃) δ 51.68, 14.27; GC-MS *m/z* 101 (C₂D₅S³⁵Cl), 103 (C₂D₅S³⁷Cl); GC-MS indicated ~100% deuteration (Fig. S2.15).

(Methylthio)methanethiol-d₅ (8-d₅). Thiourea (9.3 g, 126 mmol) was added to a solution of chloromethyl methyl sulfide-d₅ (12.5 g, 126 mmol) in dry acetone (100 mL). Cloudiness began to appear in 5 min. The solution was stored overnight at room temperature, and then cooled in ice, whereupon an oil that separated turned into a white solid. The solid was filtered and used without any further purification in the next step. (Methylthiomethyl)-d₅ isothiuronium chloride (12.5 g, 70.6 mmol) was hydrolyzed by stirring with NaOH (5 N, 2.25 eq) at room temperature for 4 h. The oil that separated as an upper layer was extracted with several portions of peroxide-free ether. The combined ether layers were washed (H₂O) and dried (Na₂SO₄). After filtration, the solvent was removed by distillation through a Vigreux column in a nitrogen atmosphere at a bath temperature of 45-50 °C affording the product as a clear, mobile liquid with a sharp, penetrating garlic-like in 40% yield; ¹H-NMR (400 MHz, CDCl₃) δ 1.94 (s); ¹³C-NMR (100 MHz, CDCl₃) δ 23.92, 13.98; *m/z* 99.0 (C₂D₅HS₂); GC-MS showed ~100% d₅ deuteration (Fig. S2.16).

2,4,5,7-Tetrathiaoctane-d₁₀ (9-d₁₀). Iodine (388 mg, 1.33 mmol) in benzene (10 mL) was added to a solution of (methylthio)methanethiol-d₅ (**8-d₅**; 250 mg, 2.66 mmol) and triethylamine (0.37 mL, 2.66 mmol) in benzene (2 mL) at 0 °C. The solution was stirred for 12 h at rt. The reaction

mixture was filtered and the filtrate was washed (H₂O) and concentrated to give **9-d₁₀** (200 mg); ¹³C NMR (100 MHz, CDCl₃) δ 45.32, 15.40; *m/z* 196.10 (C₄D₁₀S₄); GC-MS indicated ~100% deuteration (Fig. S2.17).

Associated Spectra

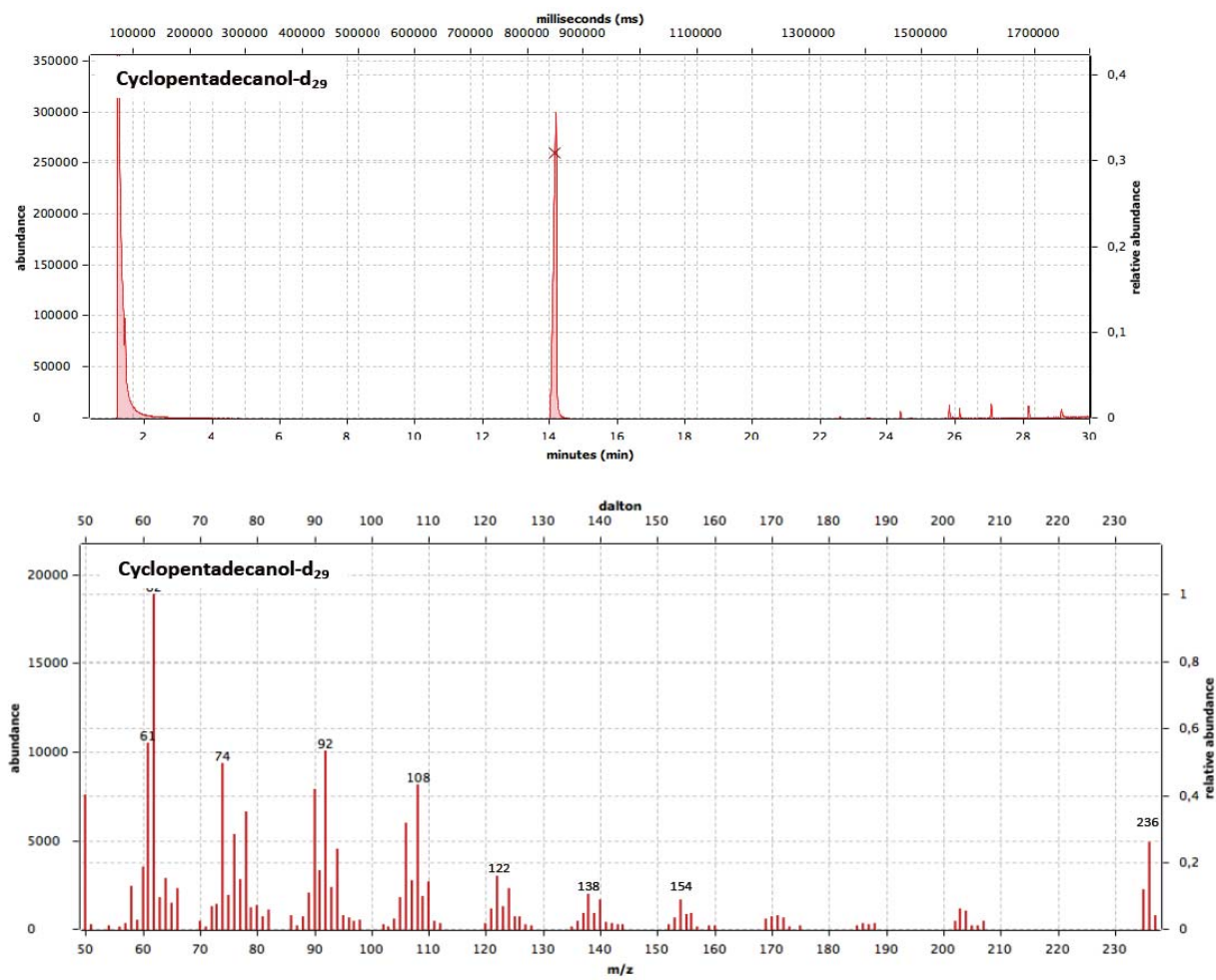


Figure S2.1 Cyclopentadecanol-d₂₉ (2-d₂₉) GC-MS.

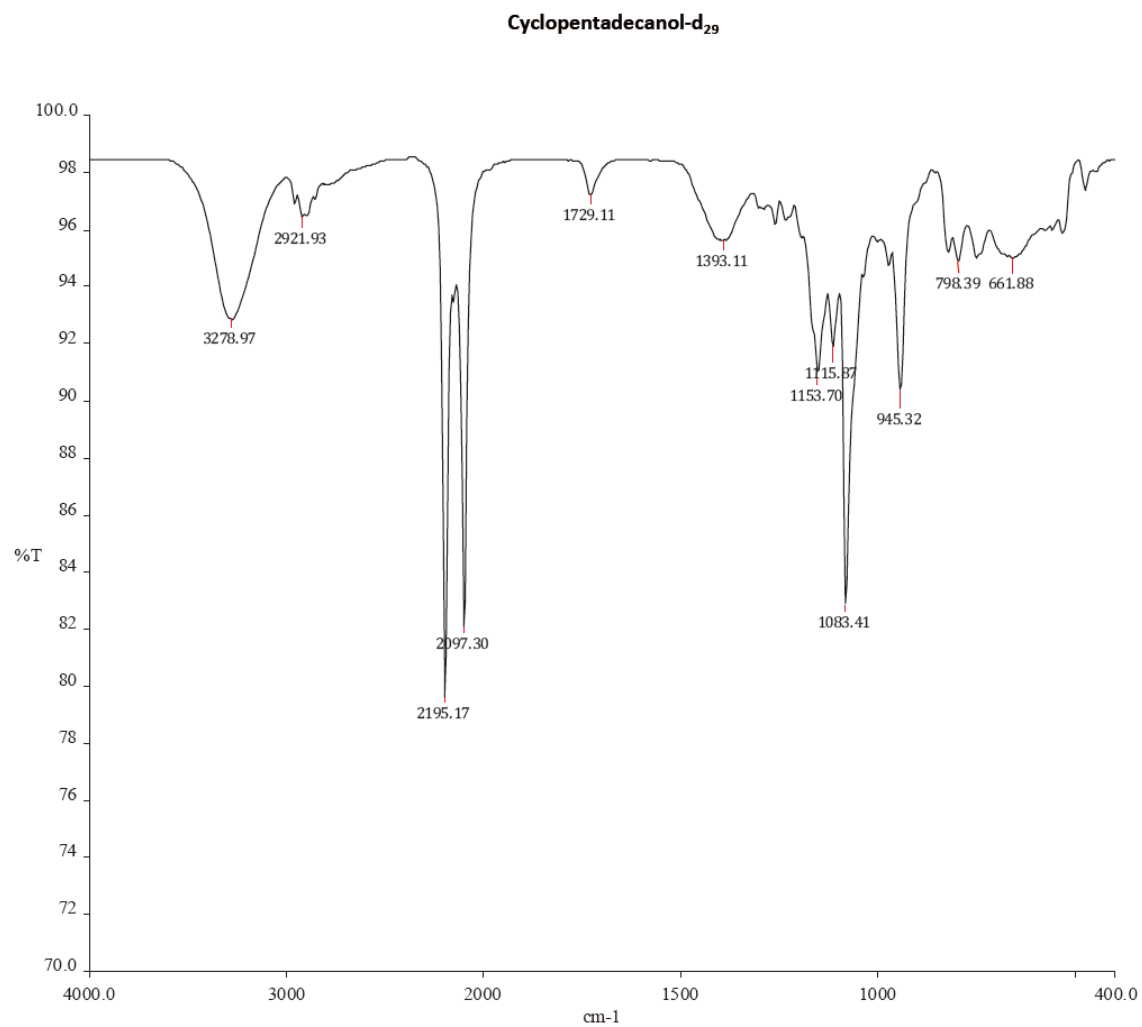


Figure S2.2 Cyclopentadecanol-d₂₉ (2-d₂₉) IR spectrum.

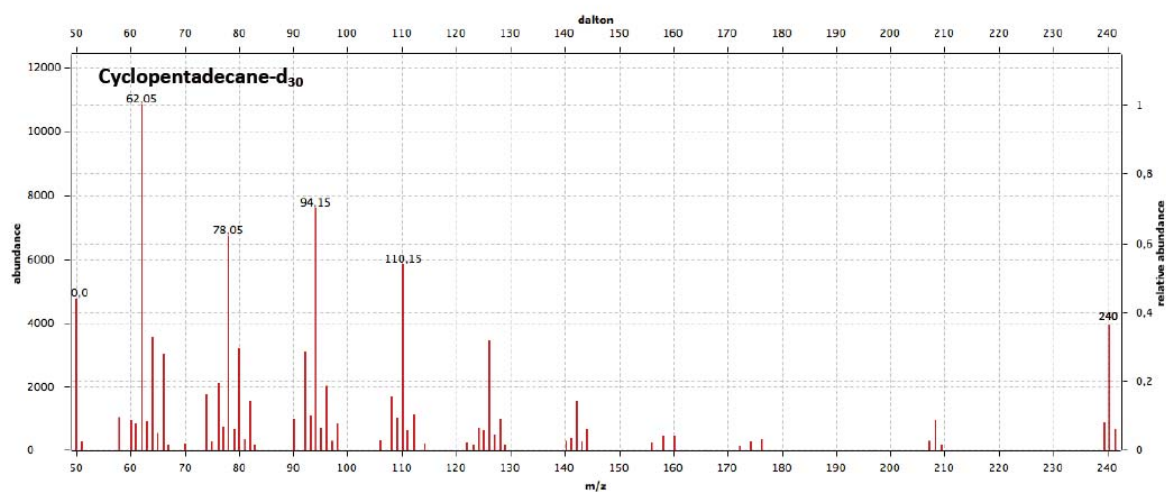
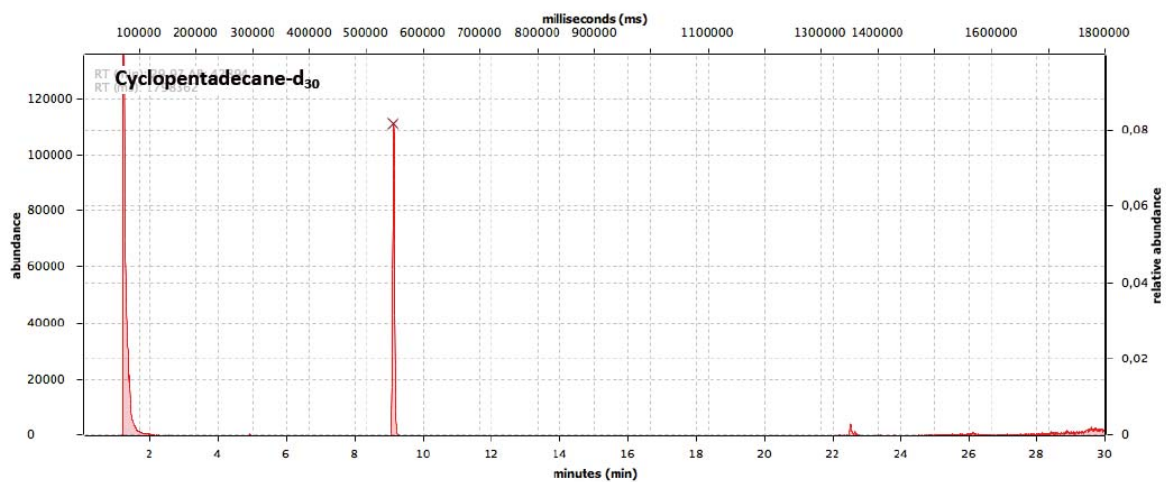


Figure S2.3 Cyclopentadecane-d₃₀ (3-d₃₀) GC-MS.

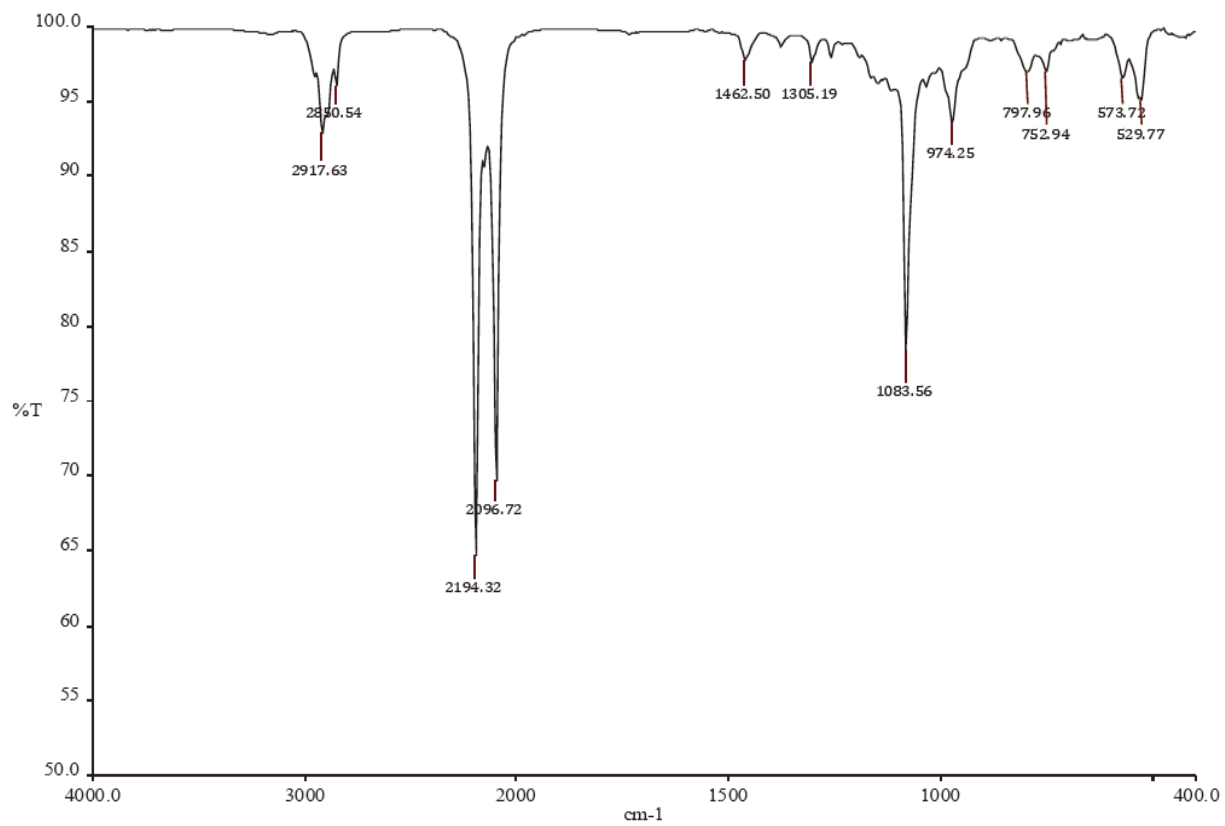


Figure S2.4 Cyclopentadecane-d₃₀ (3-d₃₀) IR spectrum.

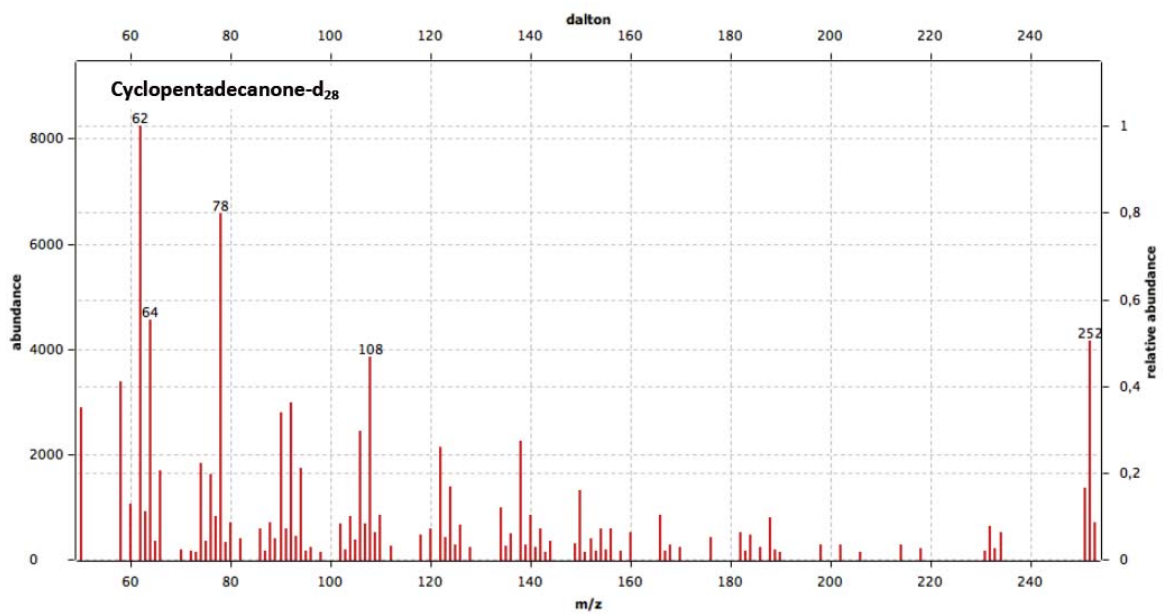
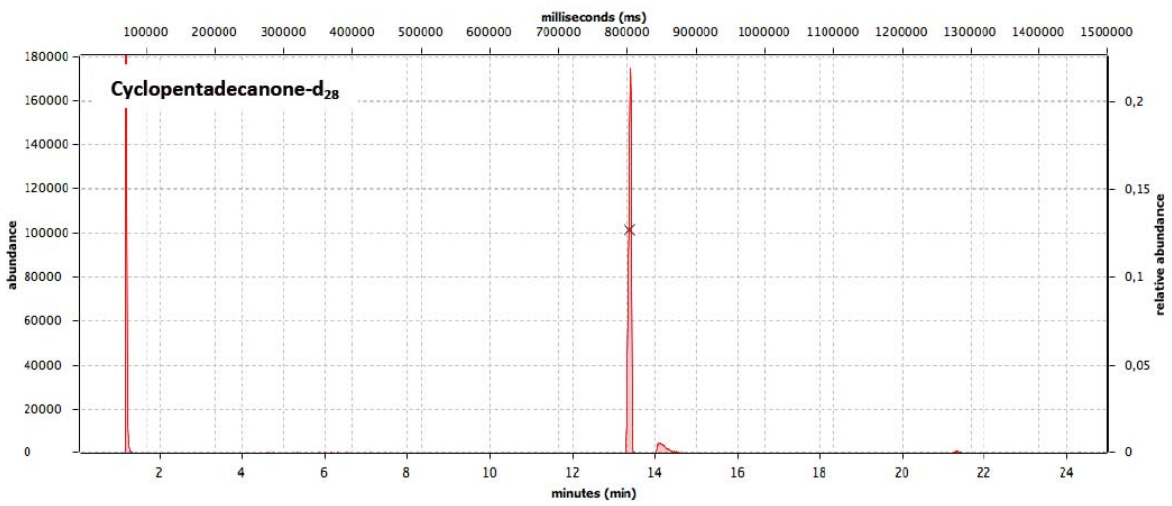


Figure S2.5 Cyclopentadecanone-d₂₈ (1-d₂₈) GC-MS.

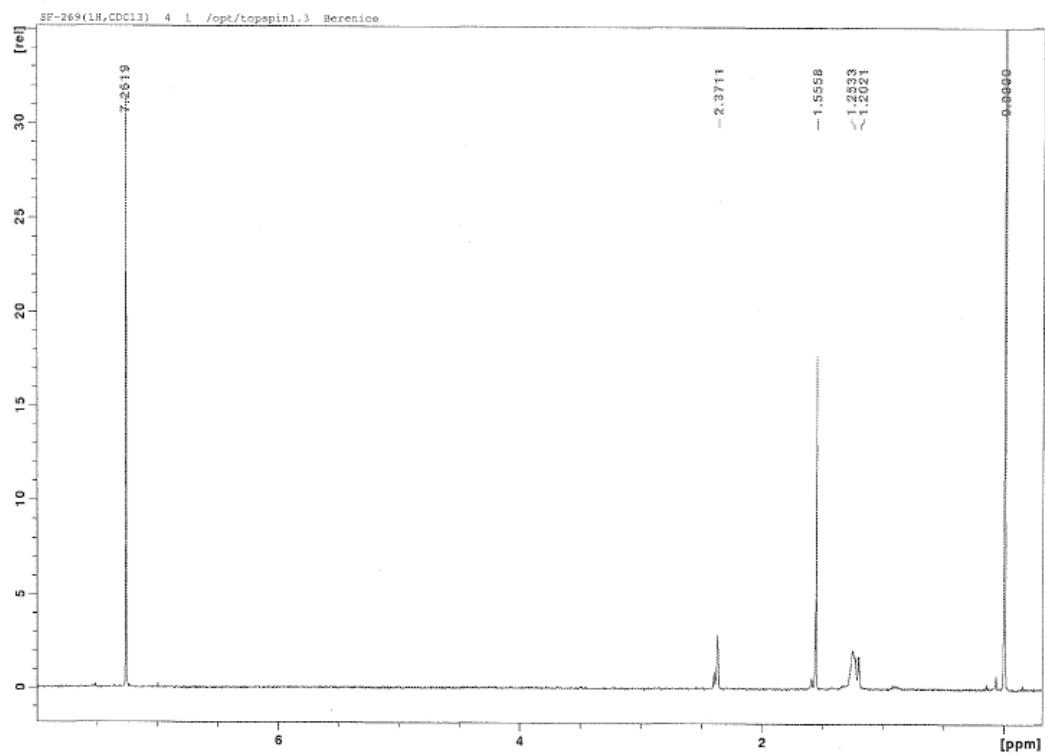


Figure S2.6 Cyclopentadecanone- d_{28} ($1-d_{28}$) ^1H NMR spectrum.

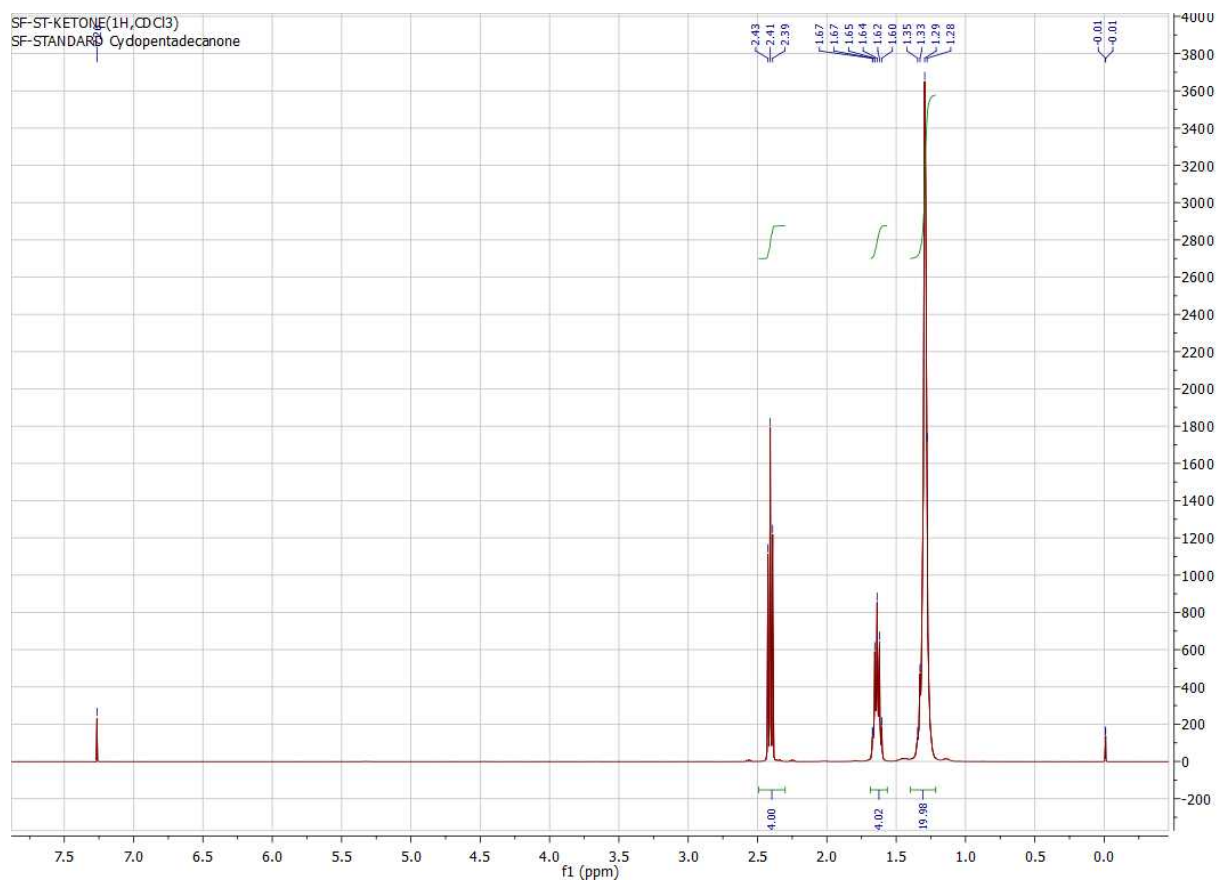


Figure S2.7 Commercial cyclopentadecanone (**1**) ^1H NMR spectrum.

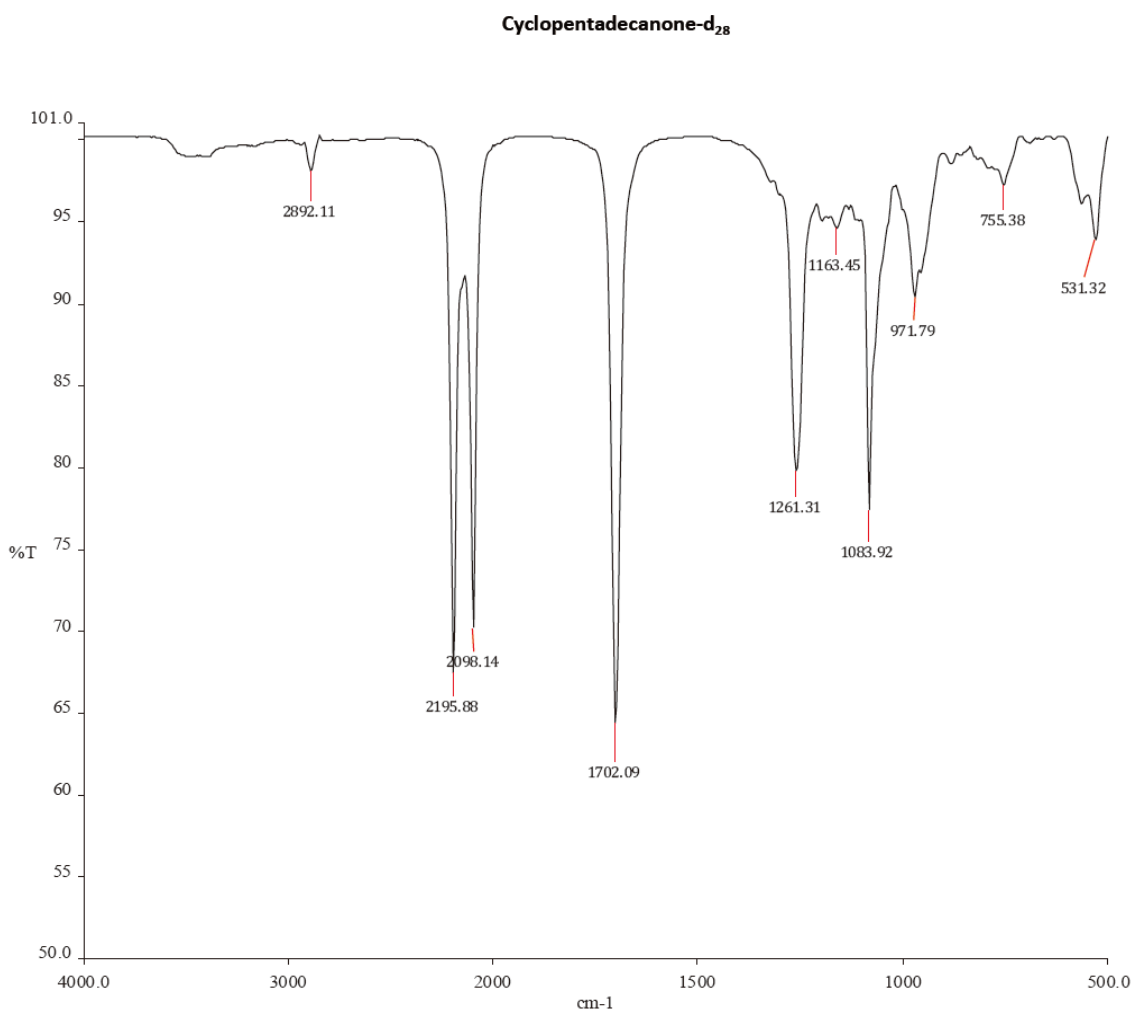


Figure S2.8 Cyclopentadecanone-d₂₈ (1-d₂₈) IR spectrum.

Cyclopentadecanone

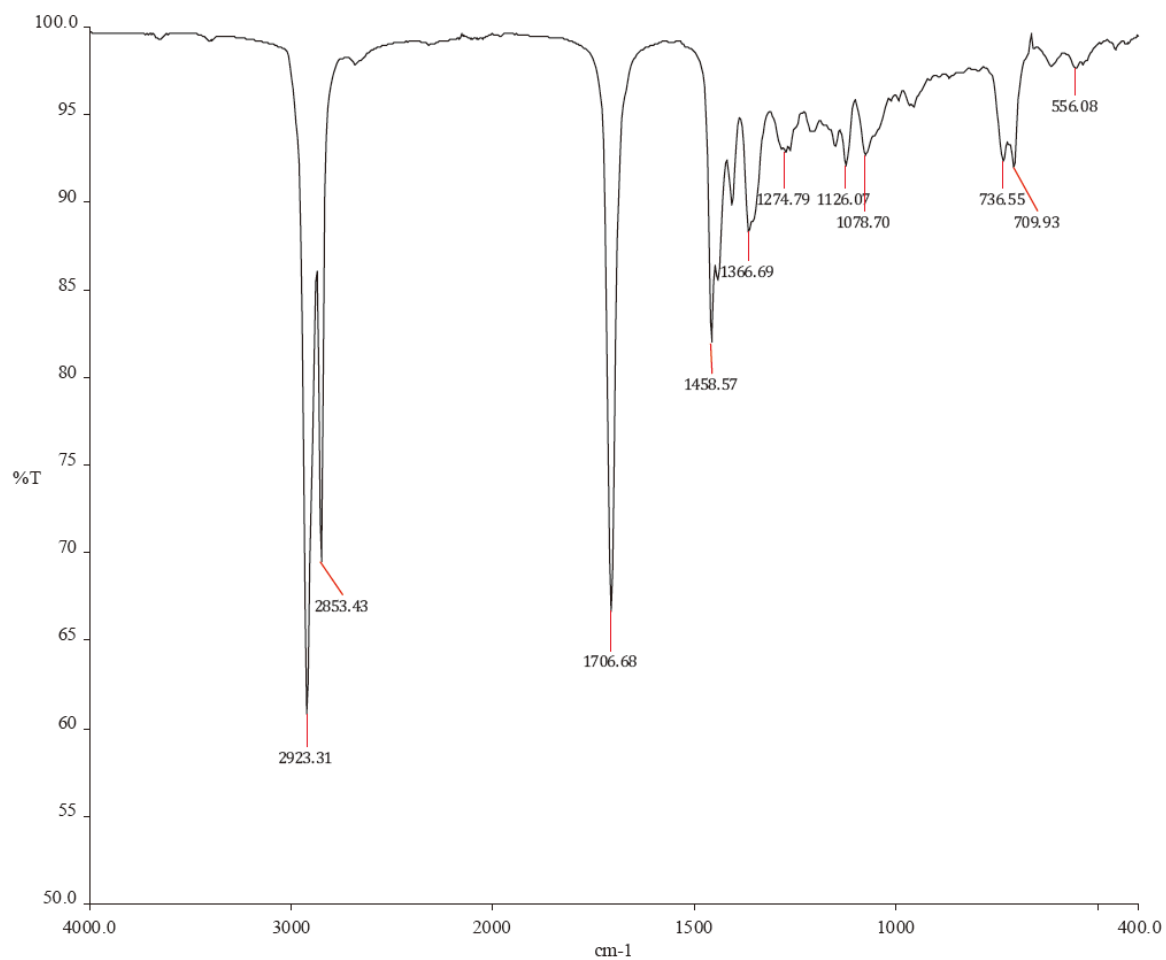


Figure S2.9 Cyclopentadecanone (commercial; **1**) IR spectrum.

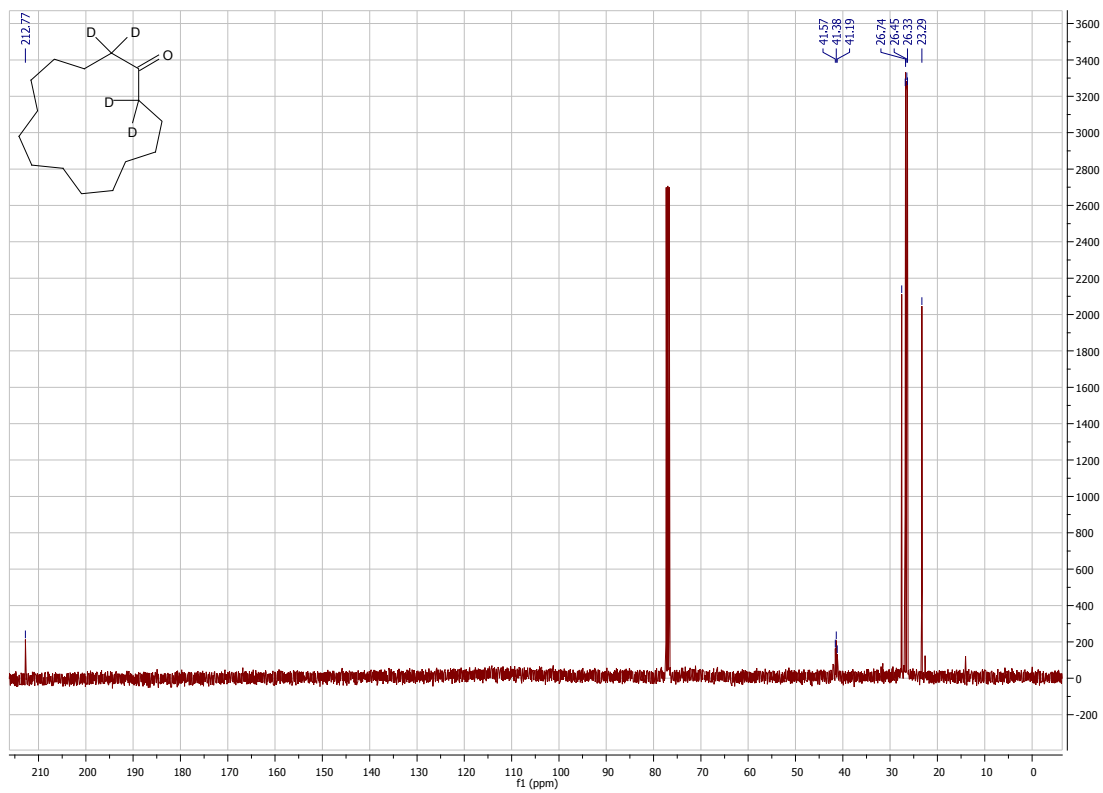
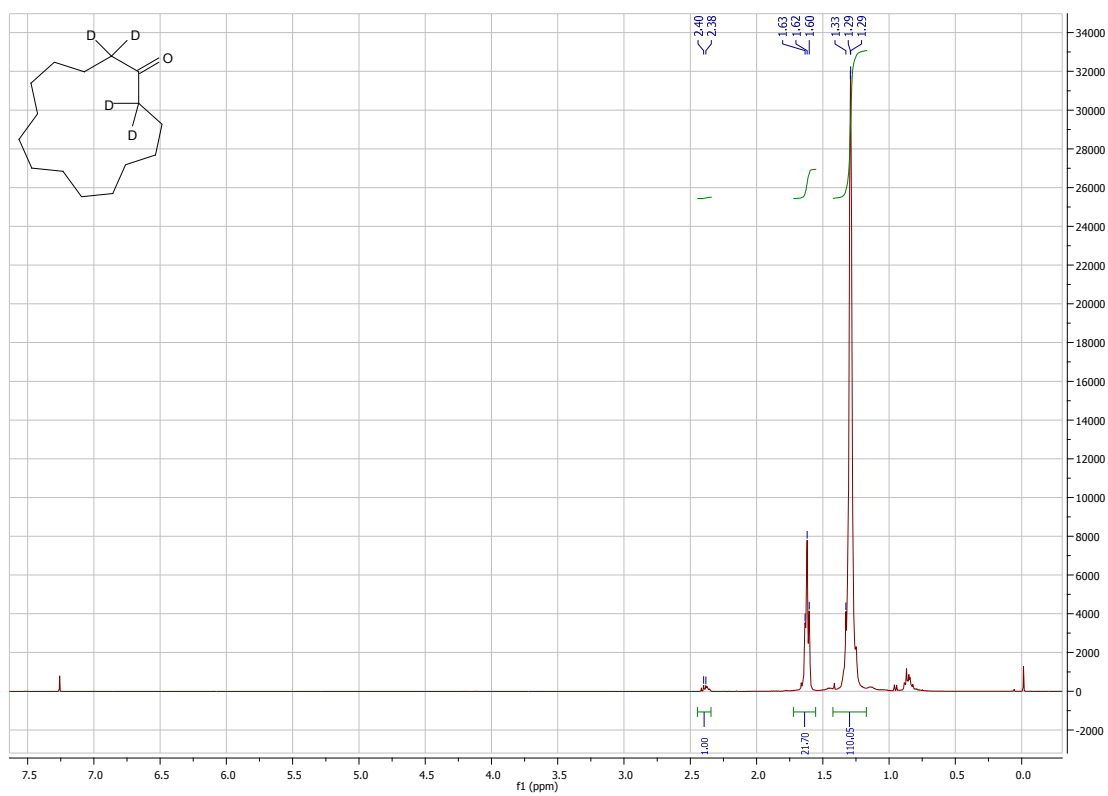


Figure S2.10 Cyclopentadecanone-2,2,15,15-d₄ (1-d₄) ¹H (top) and ¹³C (bottom) NMR spectra.

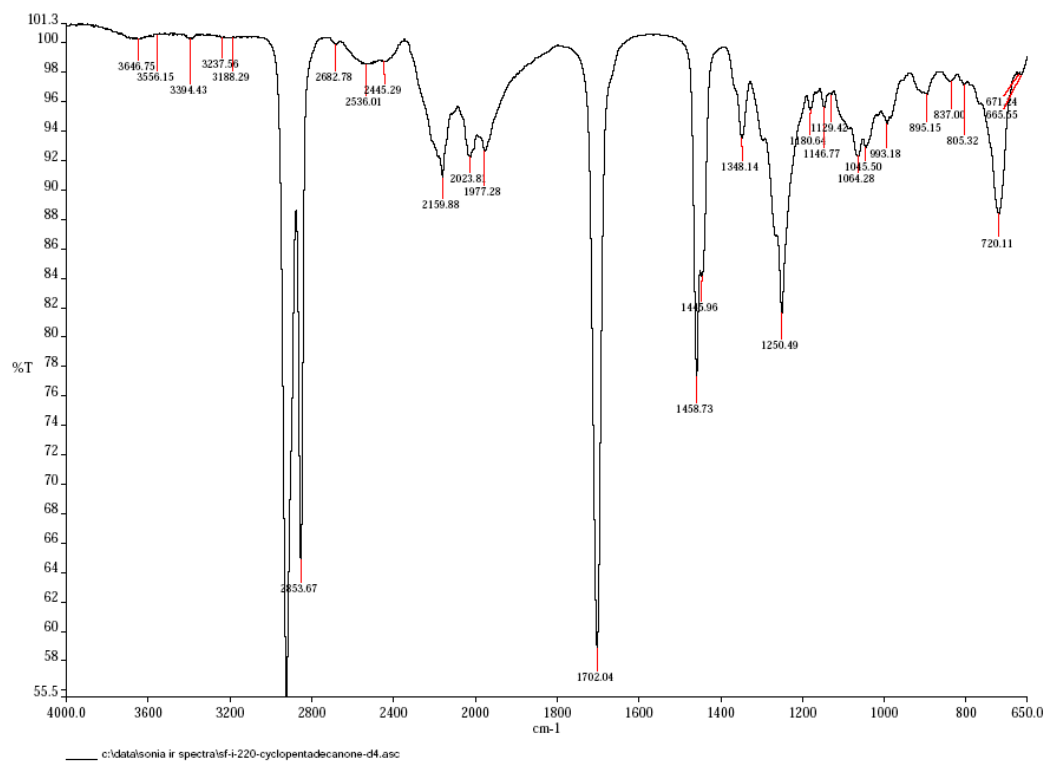


Figure S2.11 Cyclopentadecanone-2,2,15,15-d₄ (1-d₄) IR spectrum.

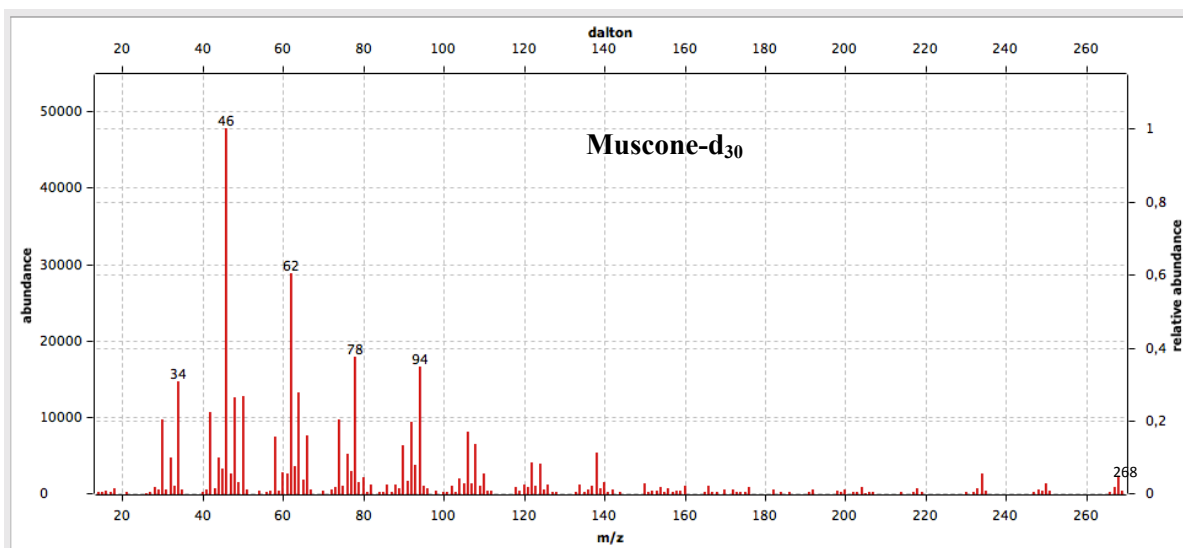
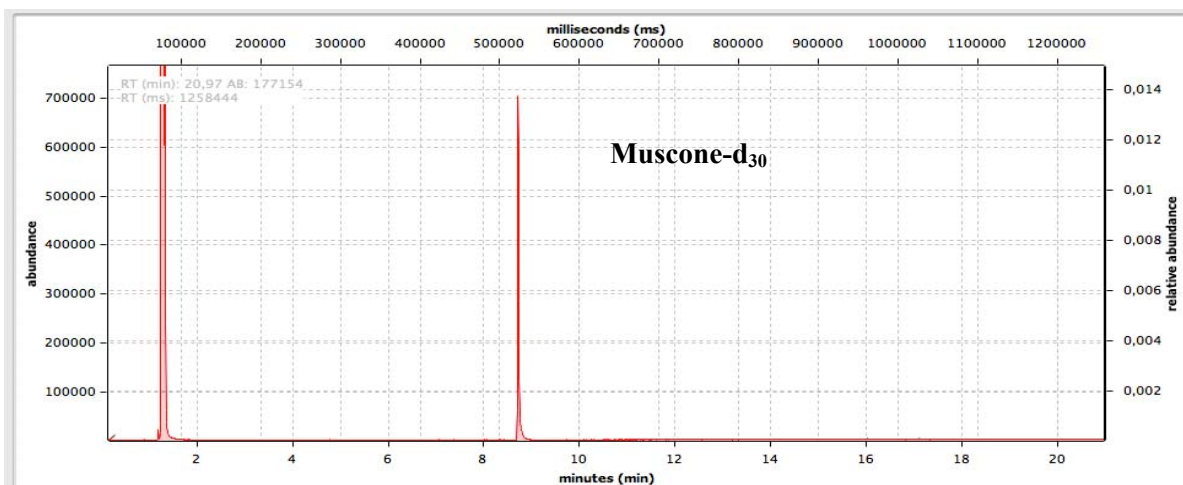


Figure S2.12 *d,l*-3-Methylcyclopentadecanone-d₃₀ (muscone-d₃₀; 4-d₃₀) GC-MS.

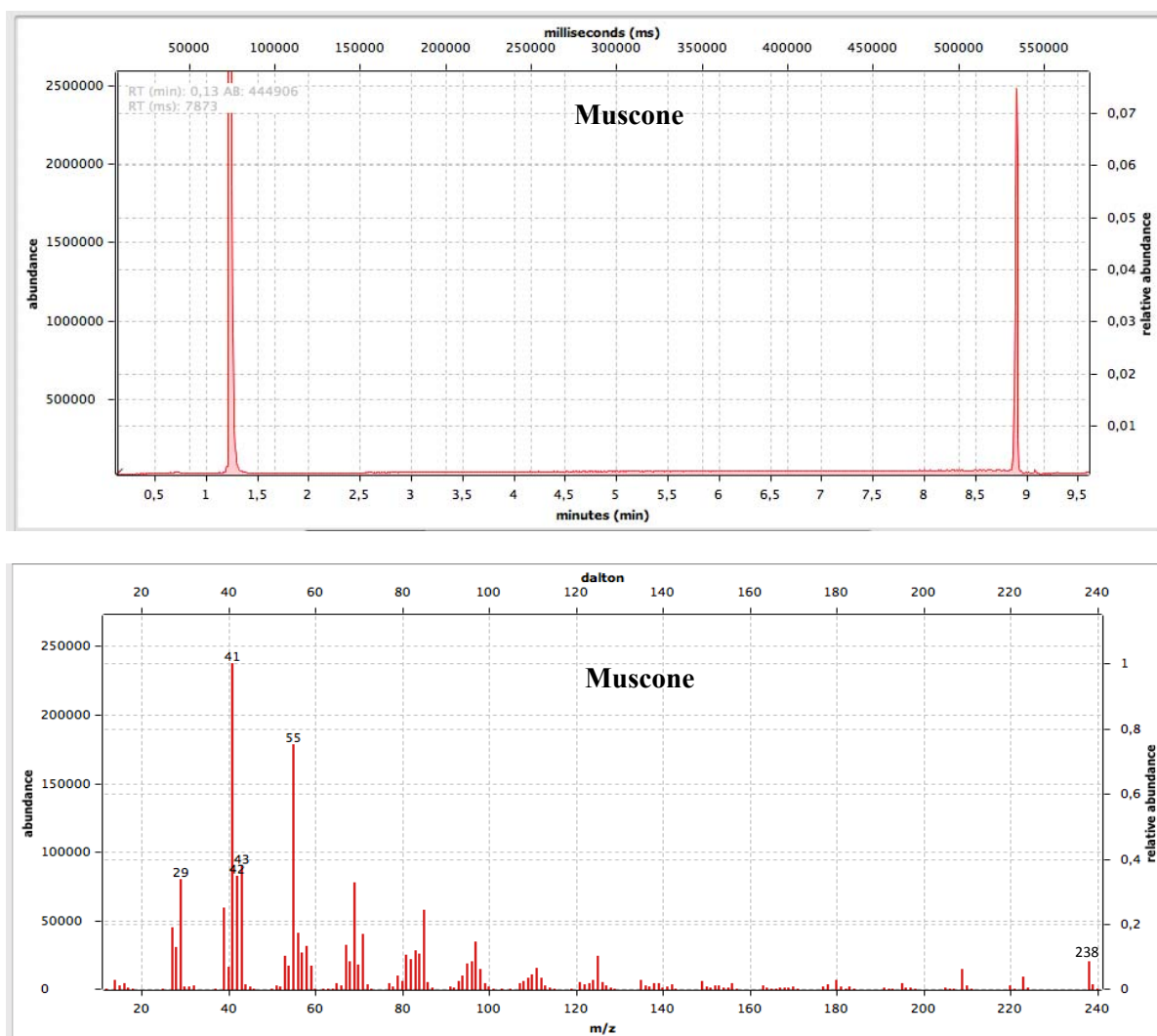


Figure S2.13 *d,l*-3-Methylcyclopentadecanone (muscone; 4) GC-MS.

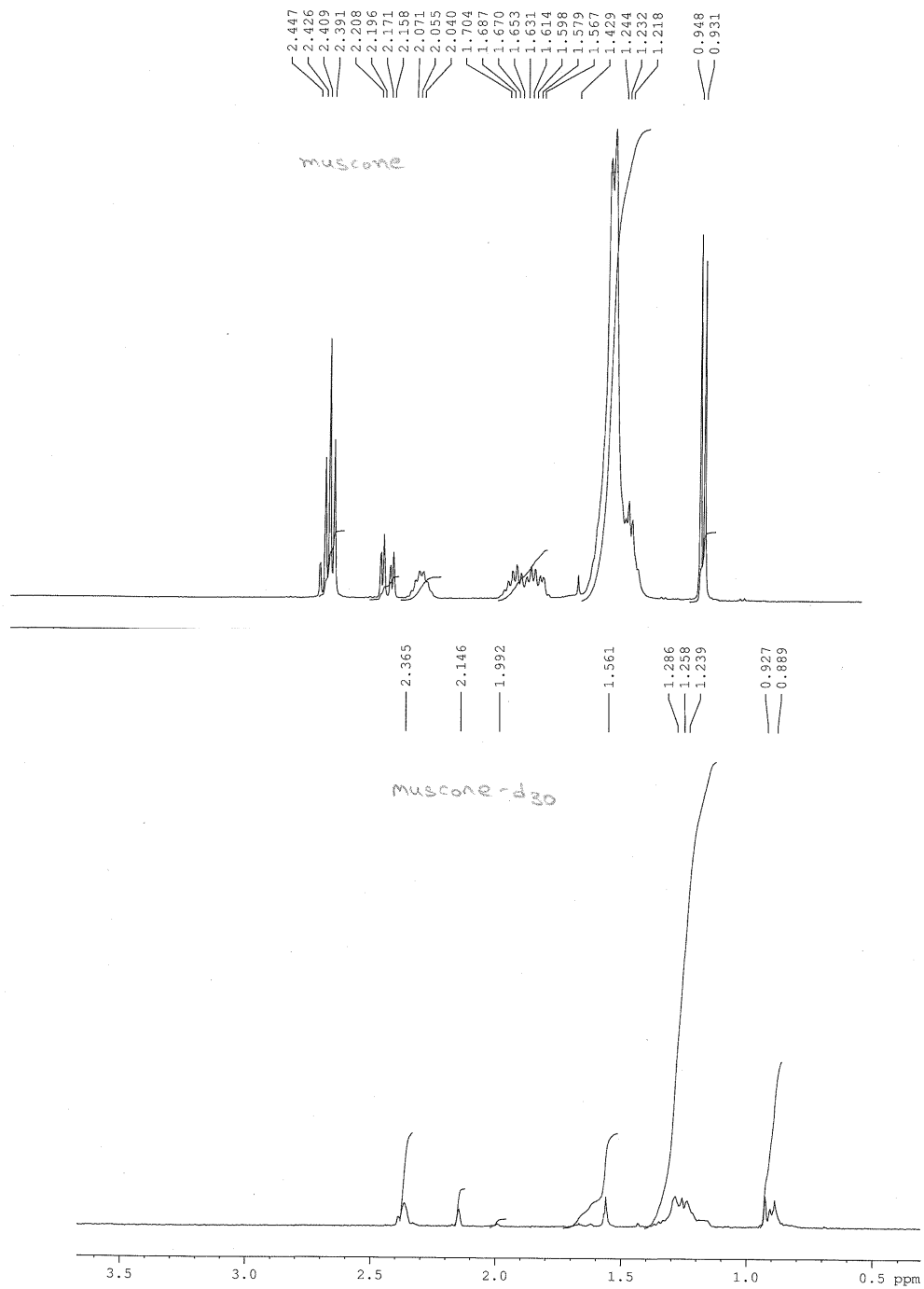


Figure S2.14 *d,l*-3-Methylcyclopentadecanone (muscone; **4**; *top*) and *d,l*-3-methylcyclopentadecanone- d_{30} (muscone- d_{30} ; **4**- d_{30} ; *bottom*) ¹H NMR spectra.

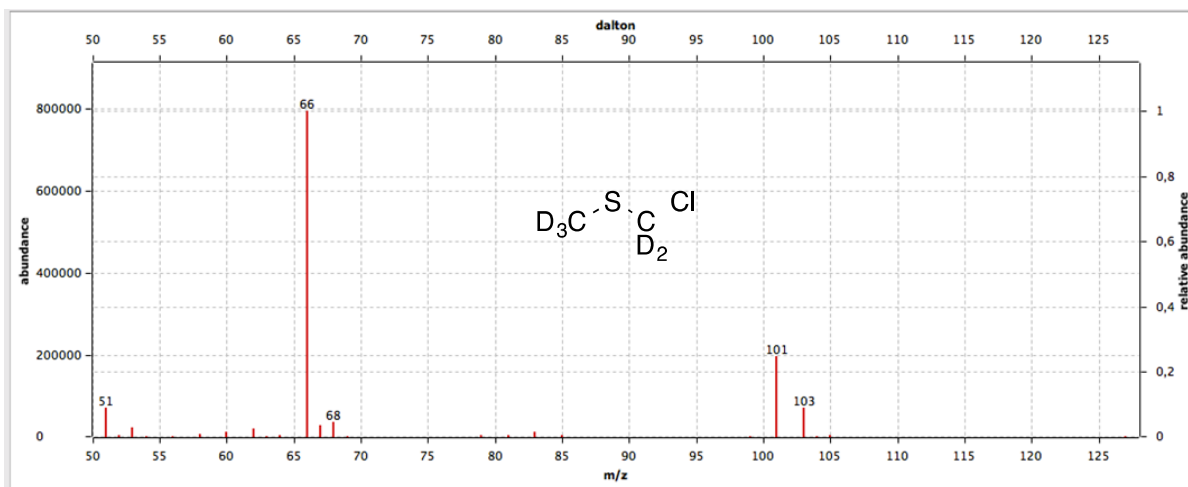
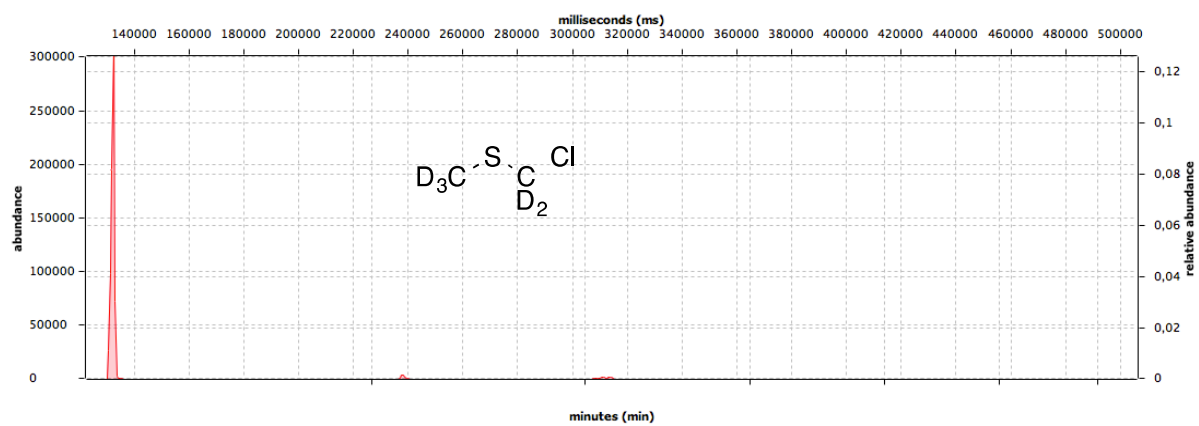


Figure S2.15 Chloromethyl methyl sulfide- d_5 .

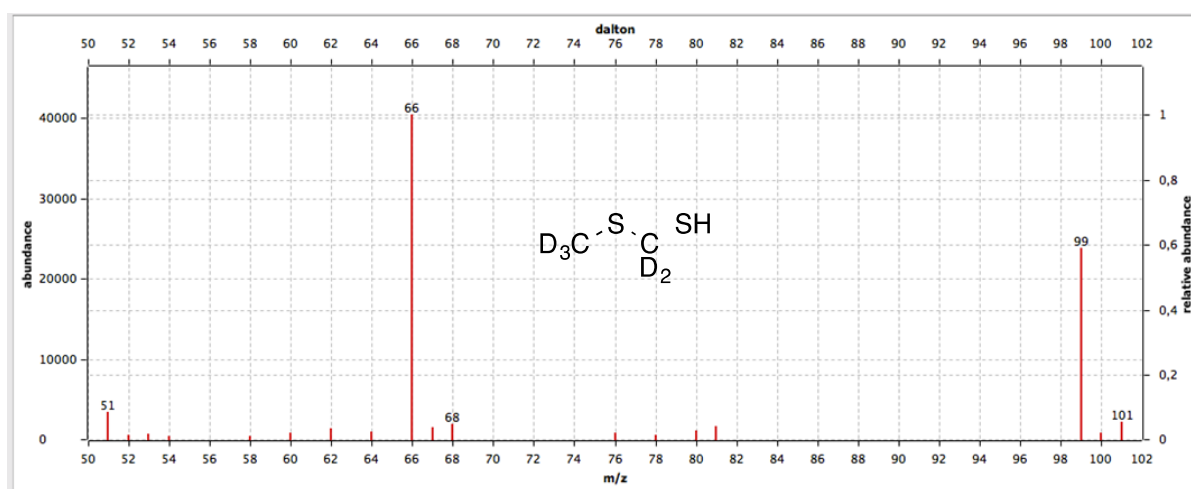
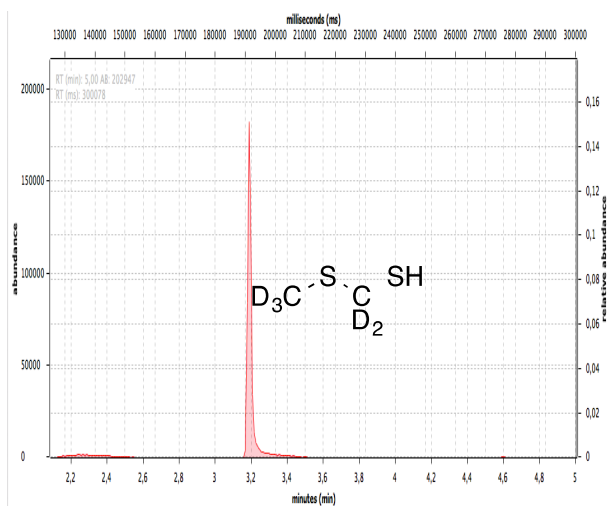


Figure S2.16 (Methylthio)methanethiol-d₅.

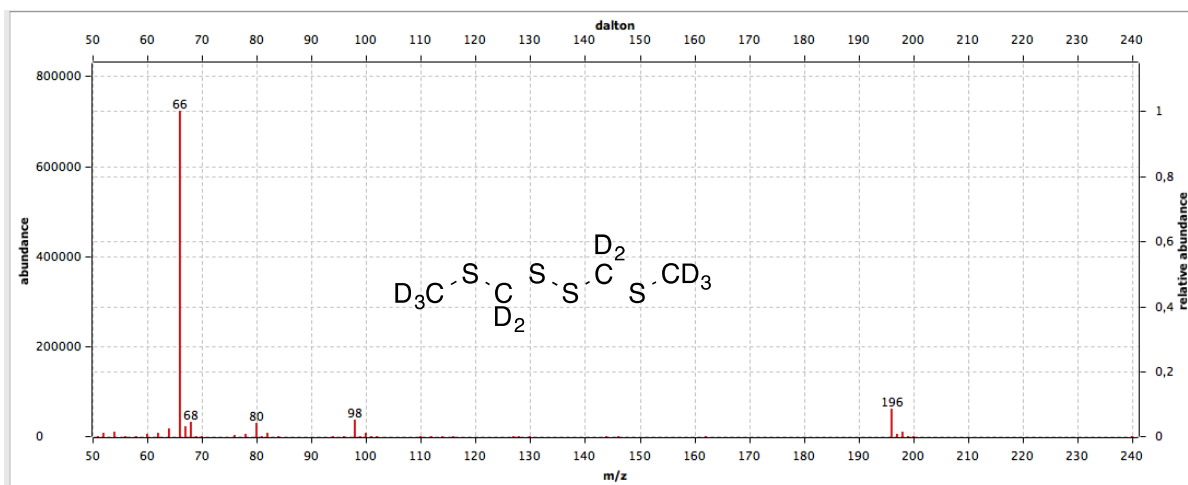
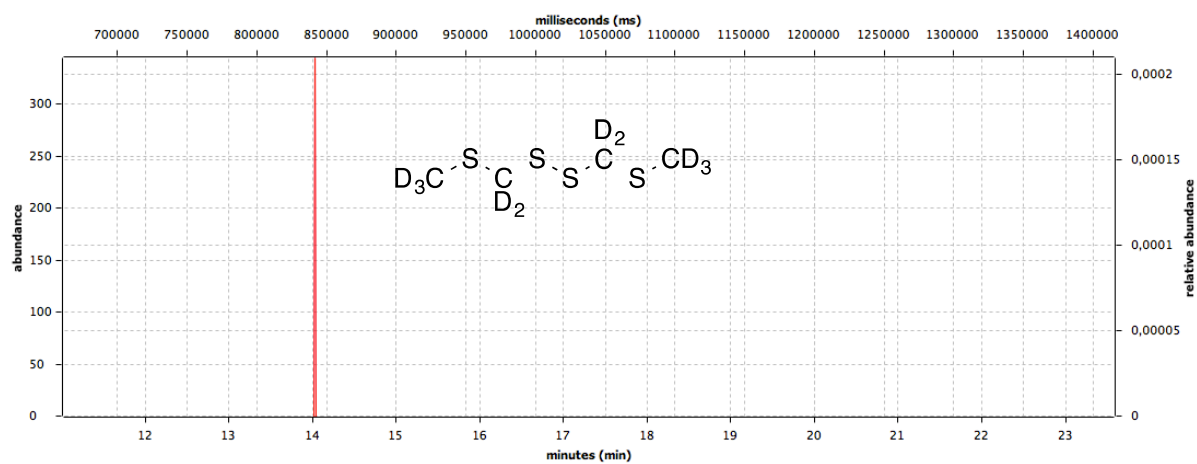


Figure S2.17 2,4,5,7-Tetrathiaoctane-d₁₀ (9-d₁₀).

Supporting Information. Part 3. Screening for human cyclopentadecanone receptor and the response of various ORs to isotopomers

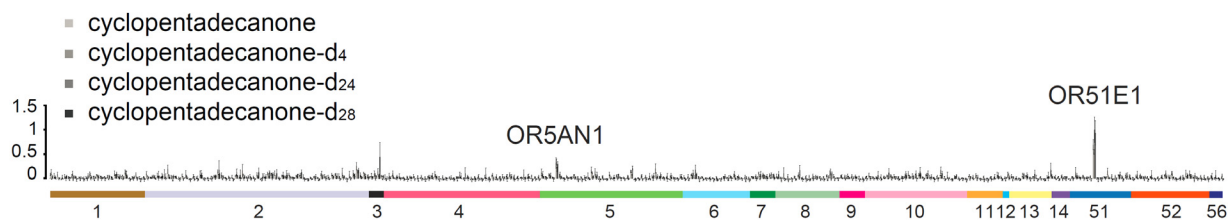


Figure S3.1. Screening for human ORs for all four isotopomers of cyclopentadecanone done using luciferase assays of 330 unique human odorant receptors. Normalized responses are shown as mean \pm S.E.M. ($N = 3$). OR51E1 was determined to be a non-responsive OR in the follow-up confirmation experiments due to a high receptor background.

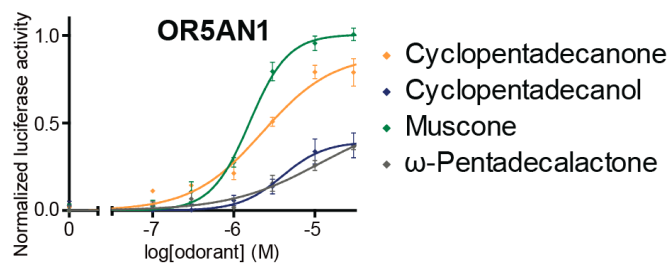
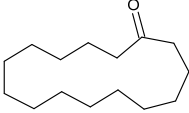
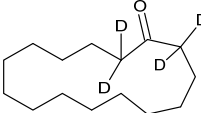
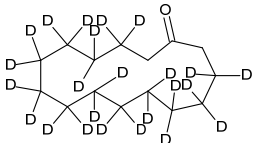
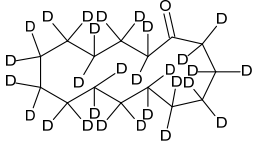
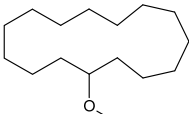
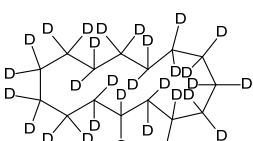
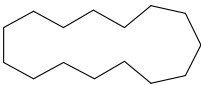
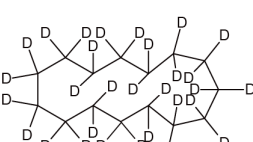
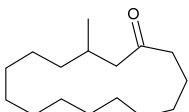
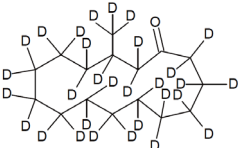
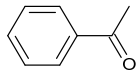
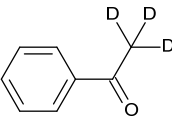
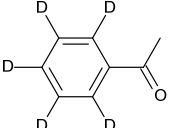
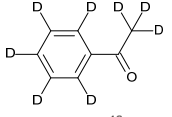
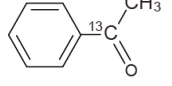
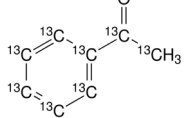
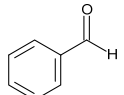
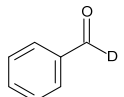
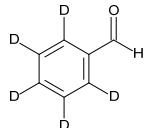
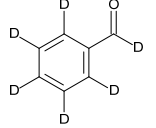
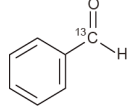
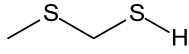
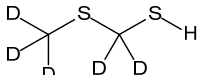
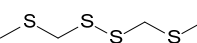
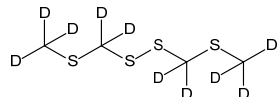
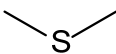
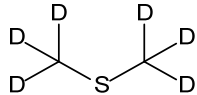
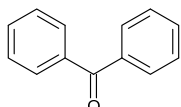
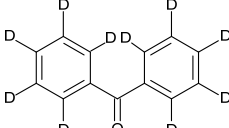
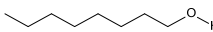
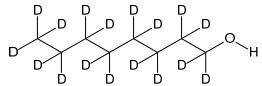
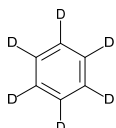
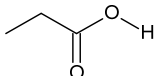
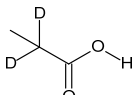
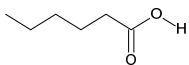
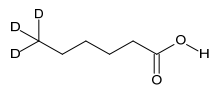
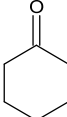


Figure S3.3. Response of human OR5AN1 to representative musk compounds, including cyclopentadecanone (**1**), cyclopentadecanol (**2**), muscone (**4**), and ω-pentadecalactone. Normalized responses are shown as mean \pm SEM ($N = 3$).

Table S3.1. A list of musk and other compounds and their isotopomers used in Figures 2 and S3.2.

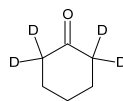
	common name	CAS No.	structure	source
1	Cyclopentadecanone (Exaltone [®])	502-72-7		Sigma-Aldrich
	Cyclopentadecanone-d ₄	N/A		In-house synthesis
	Cyclopentadecanone-d ₂₄	N/A		In-house synthesis
	Cyclopentadecanone-d ₂₈	N/A		In-house synthesis
2	Cyclopentadecanol	4727-17-7		Sigma-Aldrich
	Cyclopentadecanol-d ₃₀	N/A		In-house synthesis
3	Cyclopentadecane	295-48-7		In-house synthesis
	Cyclopentadecane-d ₃₀	N/A		In-house synthesis
4	Muscone	541-91-3		Santa Cruz

	Muscone-d ₃₀	N/A		In-house synthesis
	Acetophenone	98-86-2		Sigma-Aldrich
	Acetophenone-d ₃	17537-31-4		Chemsky
6	Acetophenone-d ₅	28077-64-7		J&K
	Acetophenone-d ₈	19547-00-3		J&K
	Acetophenone- ¹³ C ₂	190314-15-9		Sigma-Aldrich
	Acetophenone- ¹³ C ₈	N/A		Sigma-Aldrich
	Benzaldehyde	100-52-7		Sigma-Aldrich
	Benzaldehyde-d ₁	3592-47-0		Sigma-Aldrich
7	Benzaldehyde-d ₅	14132-51-5		Sigma-Aldrich
	Benzaldehyde-d ₆	17901-93-8		CDN
	Benzaldehyde- ¹³ C ₁	10383-90-1		Sigma-Aldrich
8	(Methylthio)methanethiol	29414-47-9		In-house synthesis

9	(Methylthio)methanethiol-d ₅	N/A		In-house synthesis
	Bis(methylthiomethyl) disulfide (2,4,5,7-Tetrathiaoctane)	85544-38-3		In-house synthesis
	Bis(methylthiomethyl) disulfide-d ₁₀	N/A		In-house synthesis
10	Dimethyl sulfide	75-18-3		Sigma-Aldrich
	Dimethyl sulfide-d ₆	926-09-0		Sigma-Aldrich
	Benzophenone	119-61-9		Sigma-Aldrich
	Benzophenone-d ₁₀	22583-75-1		Sigma-Aldrich
	Octanol	111-87-5		Sigma-Aldrich
	Octanol-d ₁₇	153336-13-1		Sigma-Aldrich
	Benzene	71-43-2		Sigma-Aldrich
	Benzene-d ₆	1076-43-3		Sigma-Aldrich
	Propionic acid	79-09-4		Sigma-Aldrich
	Propionic acid-d ₂	19136-91-5		Sigma-Aldrich
	Hexanoic acid	142-62-1		Sigma-Aldrich
	Hexanoic acid-d ₃	55320-69-9		Sigma-Aldrich
Cyclohexanone	108-94-1		Sigma-Aldrich	

Cyclohexanone-d₄

1006-03-7



Sigma-Aldrich

Boldface numbers in the leftmost column represent numbers used in the text.

Table S3.2. Pairwise comparisons between the dosage response curves for the original odorant and its deuterated or ^{13}C isotopomers.

A. Comparisons of dosage response curves in Figures 3 and 4.

OR	odorant	EC₅₀	F value	P value
OR5AN1	Cyclopentadecanone-H	3.49		
	Cyclopentadecanone-d ₄	4.29	1.448	17.556
	Cyclopentadecanone-d ₂₄	3.90	0.7283	36.2934
	Cyclopentadecanone-d ₂₈	3.62	0.1661	60.5616
	Cyclopentadecanone-SHAM	3.11	0.1030	63.1686
OR5AN1	Muscone-H	9.62		
	Muscone-d ₃₀	17.53	5.588	1.551
MOR244-3	(Methylthio)methanethiol	1.58		
	(Methylthio)methanethiol-d ₅	1.61	1.594	16.005
MOR244-3	Bis(methylthiomethyl)disulfide	0.21		
	Bis(methylthiomethyl)disulfide-d ₁₀	1.60	2.183	9.4314
MOR244-3	Dimethyl sulfide	4.31		
	Dimethyl sulfide-d ₆	5.55	0.6118	36.6036
MOR162-1	Acetophenone-H	6.17		
	Acetophenone-d ₃	3.99	1.722	13.4772
	Acetophenone-d ₅	5.14	0.5139	39.9894
	Acetophenone-d ₈	5.40	3.717	2.7984
	Acetophenone- $^{13}\text{C}_2$	9.15	9.221	0.099
MOR41-1	Acetophenone- $^{13}\text{C}_8$	6.13	1.357	18.4932
	Acetophenone-H	5.46		
	Acetophenone-d ₃	5.47	1.581	15.378
	Acetophenone-d ₅	3.27	0.8486	29.337
	Acetophenone-d ₈	3.41	2.909	5.3064
MOR129-1	Acetophenone- $^{13}\text{C}_2$	7.70	0.7576	31.8912
	Acetophenone- $^{13}\text{C}_8$	9.68	1.483	16.7178
	Acetophenone-H	2.29		
	Acetophenone-d ₃	2.51	0.2094	53.6448
	Acetophenone-d ₅	1.49	0.8262	29.8386
MOR271-1	Acetophenone-d ₈	0.60	7.136	0.3036
	Acetophenone- $^{13}\text{C}_2$	0.86	3.912	2.4288
	Acetophenone- $^{13}\text{C}_8$	1.19	1.431	17.325
	Acetophenone-H	32.43		
	Acetophenone-d ₃	33.54	0.04510	63.096
MOR106-1	Acetophenone-d ₅	43.91	1.022	24.9348
	Acetophenone-d ₈	40.23	0.5906	37.1778
	Acetophenone- $^{13}\text{C}_2$	57.28	4.311	1.8348
	Acetophenone- $^{13}\text{C}_8$	45.04	1.859	11.9988
	Acetophenone-H	59.35		
MOR106-1	Acetophenone-d ₃	44.32	0.8513	29.1588
	Acetophenone-d ₅	22.79	4.121	2.0922
	Acetophenone-d ₈	39.84	0.9542	26.532
	Acetophenone- $^{13}\text{C}_2$	65.61	0.04723	62.964
	Acetophenone- $^{13}\text{C}_8$	55.63	0.1664	55.9614

MOR161-1	Acetophenone-H	55.33		
	Acetophenone-d ₃	115.80	6.034	0.5874
	Acetophenone-d ₅	50.29	0.1011	59.6838
	Acetophenone-d ₈	55.31	0.04219	63.2808
	Acetophenone- ¹³ C ₂	72.06	0.5260	39.5274
	Acetophenone- ¹³ C ₈	36.12	1.797	12.6456
MOR256-17	Acetophenone-H	26.29		
	Acetophenone-d ₃	18.77	0.2532	51.4008
	Acetophenone-d ₅	20.43	0.1963	54.3378
	Acetophenone-d ₈	7.97	2.752	5.8014
	Acetophenone- ¹³ C ₂	10.22	2.131	9.5634
	Acetophenone- ¹³ C ₈	4.63	5.080	1.0824
MOR256-17	Benzaldehyde-H	15.50		
	Benzaldehyde-d ₁	13.60	0.03844	63.5184
	Benzaldehyde-d ₅	10.23	0.3895	45.0384
	Benzaldehyde-d ₆	21.09	0.3180	48.2592
	Benzaldehyde- ¹³ C ₁	20.03	0.8616	28.8816
MOR285-5	Benzaldehyde-H	11.78		
	Benzaldehyde-d ₁	7.88	7.744	0.1056
	Benzaldehyde-d ₅	6.59	4.397	1.1418
	Benzaldehyde-d ₆	18.86	3.072	3.5772
	Benzaldehyde- ¹³ C ₁	12.06	0.03876	65.307

B. Comparisons of dosage response curves in Figure S3.2.

OR	odorant	EC₅₀	F value	P value
MOR271-1	Cyclohexanone	8.79		
	Cyclohexanone-d ₄	12.68	2.371	7.8606
MOR271-1	Benzene	67.92		
	Benzene-d ₆	83.56	0.9919	27.6474
MOR31-2	Hexanoic acid	>300		
	Hexanoic acid-d ₃	>300	1.439	17.3646
MOR203-1	Octanol	2.23		
	Octanol-d ₁₇	2.47	0.03345	65.439
OR1A1	Benzophenone	9.38		
	Benzophenone-d ₁₀	8.20	0.1468	61.4064
OR2W1	Benzophenone	0.68		
	Benzophenone-d ₁₀	0.56	0.2469	56.925
OR2W1	Acetophenone-H	25.00		
	Acetophenone-d ₃	8.99	2.235	8.7846
	Acetophenone-d ₅	7.35	3.007	4.7652
	Acetophenone-d ₈	16.44	3.189	4.224
OR5P3	Acetophenone-H	39.63		

	Acetophenone-d ₃	25.53	0.5257	39.5406
	Acetophenone-d ₅	48.87	0.2926	49.467
	Acetophenone-d ₈	24.60	1.530	15.8928
OR51L1	Hexanoic acid	>300		
	Hexanoic acid-d ₃	>300	2.302	8.316
OR2J2	Octanol	>300		
	Octanol-d ₁₇	>300	2.474	6.2436
OR51E2	Propionic acid	72.44		
	Propionic acid-d ₂	62.37	0.04077	63.3666
OR5AN1	Cyclopentadecane SHAM		No curve fit	
	Cyclopentadecane-d ₃₀		No curve fit	
OR5AN1	Cyclopentadecanol-H		No curve fit	
	Cyclopentadecanol-d ₃₀		No curve fit	
	Cyclopentadecanol SHAM		No curve fit	

EC₅₀ values are given in μM. *F* values and *P* values are shown for the isotopmers compared.

Before Bonferroni correction: * *P* < 0.00076. After Bonferroni correction: * *P* < 0.05.

Supporting Information. Part 4. QM/MM binding affinity calculations of deuterated and non-deuterated MTMT

Table S4.1. ONIOM enthalpies (H) and Gibbs free energies (G) in units of Hartrees for the optimized MOR244-3 model in complex with deuterated and non-deuterated MTMT. Frequencies below 50 cm^{-1} are replaced by 50 cm^{-1} and a single imaginary frequency of $\sim 5\text{ cm}^{-1}$ has been omitted. Based on the free energies of the optimized structures, we find that both the deuterated (**8-d₅**) and non-deuterated (**8**) MTMT have similar binding affinities.

	Enthalpy	Gibbs Free Energy
MTMT	-2610.844736	-2612.336192
MTMT-d₅	-2610.860644	-2612.353322

Calculating Isotope Effects (EIEs)

Deuterium Isotope Effect

$$\begin{aligned} &= K_H/K_D \\ &= \exp [-\Delta G_H/RT] / \exp [-\Delta G_D/RT] \\ &= \exp [(\Delta G_D - \Delta G_H)/RT] \\ &= \exp [((G_D - G_H)_{\text{bound}} - (G_D - G_H)_{\text{free}})/RT] \\ &= 0.94 \text{ for MTMT} \end{aligned}$$

where “*bound*” refers to substrate bound in receptor active site and “*free*” refers to molecule as itself in gas phase. The relevant Gibbs free energy values employed for EIE calculations are presented in Table S4.2.

Table S4.2. Gibbs free energies (G) in units of Hartrees for undeuterated (G_H) and deuterated (G_D) ligand as itself (free) and bound in receptor active site (bound) with associated deuterium isotope effects (DIEs).

	G_H		G_D		DIE
	Free	Bound	Free	Bound	
MTMT	-876.088348	-2612.336192	-876.105415	-2612.353322	0.94